THE ASTROPHYSICAL JOURNAL, 447:324–341, 1995 July 1

SUPERFLUID CORE ROTATION IN PULSARS. II. POSTJUMP RELAXATIONS

A. D. SEDRAKIAN,[1,2] D. M. SEDRAKIAN,[1,2] J. M. CORDES,[1] AND YERVANT TERZIAN[1]
Received 1994 September 12; accepted 1995 January 17

ABSTRACT

A theory of nonstationary dynamics of neutron star superfluid core rotation, based on the dynamics of proton vortex clusters is presented. Exact solutions describing the postjump relaxation of the superfluid component of the star are given with allowance for the spatial dependence of viscous friction. In this theory, the core is coupled on timescales of hours to years, rather than the few seconds' coupling time in models where vortex clusters are ignored. An application of the theory to the postjump relaxations of the Vela pulsar 0833−45 shows that, within the standard range of parameters of neutron stars, the postjump relaxations of Vela can be understood in terms of the dynamics of the superfluid core. The model involves contributions to postjump relaxations from a wide range of radii, with relaxation times scaling as the square of the spin period. It is predicted that millisecond pulsars will not show timing irregularities on timescales larger than a few days.

Subject headings: dense matter — pulsars: general — pulsars: individual (Vela) — stars: interiors — stars: neutron

1. INTRODUCTION

The growing number of observations of macrojumps ("glitches") in the pulsar rotation rates and their relaxations strongly stimulates studies of superfluid dynamics in neutron stars. A macrojump in the rotation rate of a pulsar with typical amplitude $\Delta\nu/\nu \sim 10^{-8}$–$10^{-6}$ is accompanied by a jump in the spin-down rate $\Delta\dot{\nu}/\dot{\nu} \sim 10^{-2}$–$10^{-3}$. While the rise time of a jump is rather short, e.g., it is no more than 2 minutes in the case of the Christmas 1988 glitch of the Vela pulsar 0833−45 (Hamilton et al. 1989; McCulloch et al. 1990; Flanagan 1990, 1993), its relaxation timescales are observed to be from several days to several months. Moreover, recent observations with high time of resolution have made it possible to study the short term postjump response of the Vela pulsar, indicating exponential decay components with timescales of order of several hours. Less frequent macrojumps have been observed from the Crab pulsar 0531+31, with shorter postjump relaxations than those of the Vela pulsar. In the Crab's well-studied macrojump of 1989 August 29, along with the exponential decay with time constant 18 days, exponential rises on timescales 0.8, and 265 days have also been identified (Lyne, Smith, & Pritchard 1992).

Cordes, Downs, & Krause-Polstorff (1988) gave a detailed observational description of postjump relaxations of the first six macrojumps of the Vela pulsar using the data prior to 1985. They found, that a postjump relaxation process is consistent with a description assuming short rise time discontinuities in Ω and $\dot{\Omega}$ which exponentially decay with generally two distinct time constants superposed upon long-term linear decay. This analysis is independent of specific theoretical models and provides a suitable reference for model applications.

Along with the observational description of macrojump relaxations, theoretical models for these processes, involving superfluid dynamics in neutron star crusts, were developed by Alpar et al. (1984a, 1993), Jones (1990, 1992), Epstein & Baym (1992), and Link, Epstein, & Baym (1993). A number of dynamical coupling modes has been employed. In the *pinned regime*, when the superfluid velocity relaxes by means of vortex creep, the superfluid relaxation times are found to be compatible with the observed postjump relaxation timescales and the fits to the postjump data imply a realistic range of microscopic parameters (Alpar et al. 1984a, 1993; Link et al. 1993: In the model of Link et al. (1993) the relaxation times for interior temperatures $T \sim 1$–15 keV (corresponding to pulsar ages $t \geq 10^5$ yr) appear to be too large to explain relaxations observed in PSRs 0355+54 and 0525+21.

In the *free-flow* regime, the excitation of Kelvin phonons by vortex-nucleus interactions and their coupling to the thermal bath produces short relaxation times (∼seconds for the Vela pulsar) for the coupling of neutron superfluid to the crust (Epstein & Baym 1992). Thus, in this regime, crustal superfluid cannot contribute to the postjump response, but can give rise to a jump through an unpinning event. This coupling might not be effective at small vortex velocities due to localization of Kelvin phonons in the random potential of the nuclear lattice (Jones 1992). The continuum edge of the phonon spectrum cannot be reliably estimated, however. If the suppression is effective at small vortex velocities, the weak coupling mode is realized with time constants of order of 50 days (Jones 1990). Whether the free flow or the creep regimes are operative in the inner crust depends on a number of factors, like the relative orientation of nuclear and neutron vortex lattices, strength of the pinning potential, repinning timescales, etc.

In the recent theories of neutron star dynamics, a general assumption is made that the core superfluid has a negligible role in the dynamic manifestations of pulsars. In particular, it is assumed that the superfluid core is coupled to the crustal plasma and to the external braking torque on a short (unobservable) timescale due to scattering of electrons from magnetized neutron vortices (Alpar, Langer, & Sauls 1984b).

In a previous paper (Sedrakian & Sedrakian 1995, hereafter Paper I) a model of dynamical coupling of the neutron star superfluid core based on the dynamics of vortex clusters was suggested. It was shown that, owing to the strong density dependence of the free vortex flow viscosity coefficient, the core superfluid has a wide range of dynamical coupling times, which are consistent with the

[1] Department of Astronomy, Space Sciences Building, Cornell University, Ithaca, NY 14853−6801.
[2] Department of Physics, Yerevan State University, Yerevan, 375025 Armenia.

observed postjump relaxation time constants. The underlying scattering process leading to mutual friction is the scattering of relativistic electrons by the magnetic field of the vortex cluster. The viscous friction coefficient is a strongly varying function of the core density owing to the density dependence of the microscopic parameters of the problem and is independent of the core temperature.

In this paper we propose a theory of nonstationary dynamics of the superfluid core rotation that takes into account the spatial dependence of vortex friction coefficients and we provide a model for postjump relaxations based on the superfluid core dynamics. We will concentrate solely on the dynamics of the superfluid core in order to explore the capacities of the present model. As mentioned above, the possibility that crustal superfluid is coupled to the normal component on short timescales is not excluded.

Particularly, we will find solutions which describe the postjump relaxation, by summing infinite series to all orders of perturbation theory with respect to the small parameter assumed in the problem—the ratio of the moment of inertia of the superfluid region to that of the normal matter and the superfluid matter that is tied rigidly to it. (Results in the second order of perturbation expansion have been given in Sedrakian & Sedrakian 1992).

When viscous friction is position independent, the theory contains the limit which is identical to the two component model first developed by Baym et al. (1969), and Ruderman (1969) and further elaborated by Ruderman & Sutherland (1974), Greenstein (1975), Krasnov (1977), Bildsten & Epstein (1989), and Jones (1990). However, note that, in constrast to the original two-component theory of Baym et al., which was based on the idea of weak coupling of superfluid vortices to the normal component, here the strong coupling limit is relevant due to the vortex clusters' scattering of electrons. (For more details see § 2 and Paper I). Dynamical equations that include spatial dependence of mutual friction in the context of vortex creep theory in the crust have been elaborated by Cheng et al. (1988).

The plan of the paper is following. In § 2 we briefly review the vortex cluster model. In § 3 we give the basic equations describing the dynamics of the superfluid core with the allowance of spatial dependence of the viscous friction coefficients. In § 3.2 the microjump relaxation process of the superfluid core is considered. Exact solutions of the postjump relaxation of the rotation frequency and the spin-down rate are found in the limit where the ratio of the moment of inertia of the superfluid region involved in the postjump relaxation to that of the regions coupled to the normal matter on short timescales is small. A comparison with the observed postjump relaxations of the Vela pulsar is made in § 4, while the implications of the model for the production of a macrojump are discussed in § 5. The marcojump processes in pulsars other than Vela are discussed and compared with the model calculations in § 6. Finally a summary of results and conclusions are presented in § 7.

2. VORTEX CLUSTERS AND DYNAMICAL COUPLING TIMES

An important consequence of the mutual coupling of neutron and proton condensates via the entrainment effect is that the superfluid circulation of neutron vortex lines induces entrainment currents of superfluid protons, which generate local magnetic fields, around the neutron vortex lines.

Since protons in the quantum liquid region form a type II superconductor, the normal–superconducting matter interface energy is negative and at certain values of local magnetic fields, ($H > H_{c1}$, H_{c1} being the lower critical field), it is energetically favorable for unentrained protons to go over to the mixed state, by forming a lattice of vortices. The local magnetic field intensities produced by the entrainment currents, generate a cluster of proton vortices around each neutron vortex line in a region of size

$$\delta_n = \left(\frac{\xi_p}{\delta_p}\right)^{1/2|k|} d_n , \tag{1}$$

thus giving rise to an axially symmetrical induction field within the cluster:

$$\langle \boldsymbol{B} \rangle = \mu \langle \boldsymbol{v}_p \rangle \frac{\Phi_1}{4\pi\delta_p^2} , \tag{2}$$

where d_n is the size of a neutron vortex, $\xi_p = \hbar^2 k_{Fp}/\pi m_p^* \Delta_p$ is the coherence length of unentrained proton condensate, which determines the lengthscale at which the superconducting pair correlation breaks down, and the normal vortex core of bound quasi-particles is formed, k_{Fp} is the Fermi wavenumber of unentrained protons, Δ_p is the proton superconducting gap. Here $\Phi_1 = |k|\Phi_0$, $k = (m_p^* - m_p)/m_p$ is the entrainment coefficient, m_p^* and m_p being the proton effective and bare masses, respectively, Φ_0 is the flux quantum, μ is the effective magnetic permeability of the vortex cluster, $\delta_p = (m_p^* c^2/4\pi e^2 n_p)^{1/2}$ is the magnetic field penetration depth, and n_p is the number density of protons.

Energetically, the most favorable proton vortex lattice structure, as in the case of laboratory type II superconductors, is the triangular one, with the intervortex spacing $d_p^2 = (2\Phi_0/3^{1/2}\langle B \rangle) \sim 10^3$ fm. Note that the characteristic size of proton vortices are of order of the magnetic field penetration depth, $\delta_p \sim 100$ fm, and are extremely small, compared to the neutron vortex size, $d_n \sim 10^{-4}$–10^{-3} cm.

The size of the vortex cluster is macroscopic, $\delta_n \sim 10^{-5}$ cm; however, it is typically an order of magnitude smaller than the neutron vortex size, d_n, and is naturally constrained by the condition that the protons form a type II superconductor, (see eq. [1]). Beyond the cluster, in the region $\delta_n \leq \zeta \leq d_n$, the magnetic field produced by the entrainment currents, is smaller than the lower critical field, H_{c1}, and therefore it is screened by the superconducting Meissner currents of unentrained protons.

The net number of proton vortices in a cluster is $\langle n_p \rangle = [\langle B \rangle/\Phi_0]\pi\delta_n^2$, or using equation (2),

$$\langle n_p \rangle = \mu \frac{|k|}{4} \left(\frac{\delta_n}{\delta_p}\right)^2 , \tag{3}$$

which is of order of 10^{12}–10^{13} for typical values of parameters $\mu \sim 2$ and $|k| \sim 0.2$–0.3. A sketch of a vortex cluster is shown in Figure 1.

The interaction between the vortex clusters and the electron fluid is dominated by the process of magnetic scattering of relativistic electrons by the magnetic field of the vortex cluster. The viscosity coefficient, η, for this process is (Paper I)

$$\eta = \frac{\pi}{\sqrt{3}\,128}\,\frac{\hbar}{\delta_p^3}\,\frac{k_e^2}{n}\,\mu|k|\left(\frac{\xi_p}{\delta_p}\right)^{1/|k|}, \tag{4}$$

where k_e is the Fermi wavenumber of electrons and n is the density of vortex clusters. This expression was derived assuming that the neutron vortices and the proton vortices that are bound in the cluster form a triangular two-dimensional lattice in the plane perpendicular to the rotation axis.

As derived in § 3 the *dynamical relaxation times* of the superfluid are given in terms of the friction coefficient as

$$\tau_d = \frac{1}{2\omega_s(0)}\,\frac{\eta}{\rho_s^* v}\left[1 + \left(\frac{\rho_s^* v}{\eta}\right)^2\right], \tag{5}$$

where ρ_s^* is the effective superfluid density, $v_n = \pi\hbar/m_n$ is the quantum of circulation, and $\omega_s(0)$ is the initial superfluid angular velocity (see eq. [44] below). For the present model the strong coupling condition $\eta \gg \rho_s^* v_n$ is satisfied. Then, substituting equation (4) in equation (5), one finds

$$\tau_d = \frac{\sqrt{3}\pi}{2048}\,\frac{\hbar}{m_e}\,\frac{\rho_e}{\rho_s^*}\,\frac{1}{k_e\delta_p^3}\,\mu|k|\left(\frac{\xi_p}{\delta_p}\right)^{1/|k|} P^2\,. \tag{6}$$

where ρ_e is the electron density, m_e is the electron mass and P is the spin period. The dynamical relaxation time τ_d is a strongly varying function of the matter density, mainly due of the factor $(\xi_p/\delta_p)^{1/|k|}$, which scales as the third to fifth power of ξ_p/δ_p. This

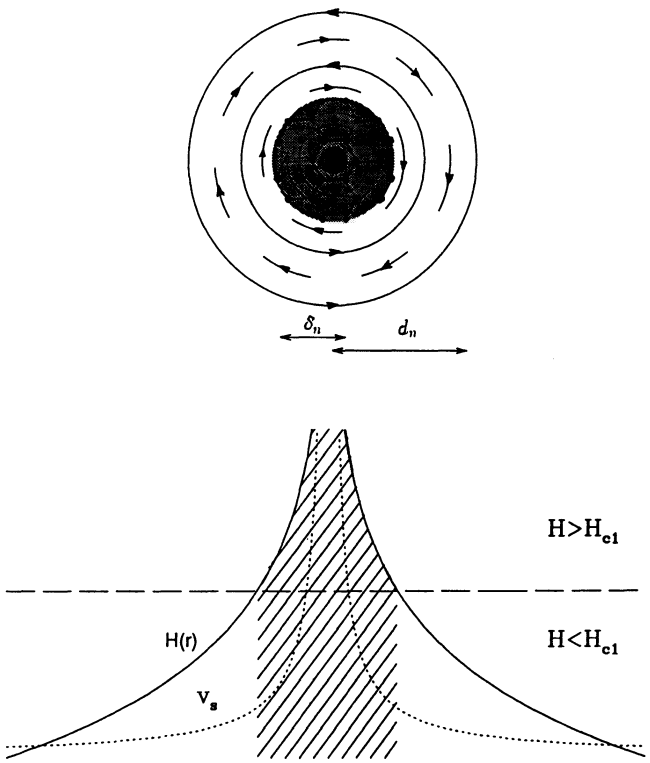

FIG. 1.—Sketch of a vortex cluster. *Upper panel:* the concentric solid circles represent the streamlines of neutron superfluid circulation around the neutron vortex core; the dashed circles represent the streamlines of the *entrained* proton superfluid, which is coupled to the neutron superfluid circulation due to the strong nuclear neutron-proton interaction. Note that the neutron and proton steamlines are oppositely directed, since the entrainment coefficient, $(m_p^* - m_p)/m_p$, is negative for typical parameters of proton superconductor. The size of the neutron vortex is determined by the spin period of pulsar as $d_n = [\hbar/2(3)^{1/2}m_n]^{1/2}P^{1/2}$ and is e.g., 4×10^{-3} cm for the Vela pulsar with period $P = 0.089$ s. The shaded region is the region where the magnetic induction created by entrained proton supercurrents is larger than the lower critical field, H_{c1}, and therefore the formation of proton vortex lines is energetically favorable. The size of this region, δ_n, is found from the condition $H(r) = H_{c1}$. Typically $\delta_n \sim 10^{-5}$ cm. The triangular proton vortex lattice in this region is shown schematically: the size of a single proton vortex line is $\delta_p \sim 10^{-11}$ cm, while the intervortex distance is $d_p \sim 10^{-10}$ cm. *Lower panel:* The generated magnetic induction $H(r)$, which falls from the center of the neutron vortex line logarithmically, is shown by the *solid line*. The *short-dashed* line is the neutron superfluid velocity, falling from the center of the neutron vortex line as $v_s(r) = \hbar/2m_n r$. The *long-dashed* line corresponds to $H(r) = H_{c1}$. The hatched region is the region where $H(r) > H_{c1}$ and the generation of proton vortices is energetically favorable.

factor is associated with the number density of proton vortices within a cluster. Note that τ_d is temperature independent, but depends quadratically on spin period.

Quite generally, when the dynamical coupling of superfluid to the normal matter is due to the scattering of normal quasiparticles from the neutron vortices, the relaxation timescale, τ_m for the underlying microscopic process is inversely proportional to the density of neutron vortices and therefore is proportional to P. Consequently, η, which is related to τ_m by the relation $\eta = (\hbar k_e/m_e c\tau_m)(\rho_e/n)$, is independent of P and one finds that $\tau_d \sim P$. This is the case in both limits of strong- and weak-coupling, and is found for different processes in the past studies, (see Sauls, Stain, & Serene 1982; Alpar et al. 1984b).

In the case of vortex cluster friction one finds a different dependence, $\tau_d \sim P^2$, which follows from the fact that electrons are scattered by the proton vortices bound in a cluster. The mean density of proton vortices is independent of the rotation period. Indeed, if the star is spinning down, the neutron intervortex spacing increases; however the region where the appearance of proton vortices is energetically favorable increases too, in a way such that the net number of proton vortices (and the axially symmetrical magnetic induction) within the superfluid core remains unchanged. An observational study of $\tau_d(P)$ dependence for different pulsars assuming that the same superfluid regions are involved in the postjump relaxations may allow us to distinguish the postjump relaxation according to the present model from models mentioned above. This topic is discussed in more detail in § 6.

In the remainder of this section we will give a brief qualitative discussion of the stability of the ground state. The ground state vortex configuration can be affected when a nonequilibrium state is imposed. First, a cluster moving with velocity v_L will induce a mean electric field,

$$\langle E\rangle = -c^{-1}[v_L \times \langle B\rangle] = -\frac{\mu\Phi_1}{4\pi c\delta_p^2}[v_L \times \langle v_p\rangle] . \tag{7}$$

For typical vortex cluster velocities $v_L/c \ll 1$, the change in the electromagnetic energy density due to the electric field is of order $(v_L/c)^2$, and therefore is negligible. Second, the quasi-equilibrium solutions of dynamic equations imply quasi-equilibrium departures between the electrons and neutron superfluid. The magnetic field intensities associated with the entrained proton condensate then may exceed the lower critical field H_{c1}, and the unentrained proton condensate can be unstable against formation of additional proton vortices. Any increase in the mean number of proton vortices will increase the friction, ($\eta \propto \langle n_p\rangle$), and consequently the departure, which in its turn will imply further increase of $\langle n_p\rangle$. Whether this kind of instability can develop or not depends on the magnitude of the critical fluctuation for creating a seed of a mixed phase in a nonequilibrium situation. The increase of the number of proton vortices will stop, when the mean free flight time for microscopic scattering of electrons of the vortex clusters, τ_{eC}, will become smaller than the electron-electron relaxation timescale, τ_{ee}. Indeed, when $\tau_{eC} < \tau_{ee}$ the introduction of the electron fluid as the normal component of the mixture, with certain velocity, v_e, is meaningless. Under these conditions the mutual friction in the bulk of the system is absent, and it behaves like a solid state crystal in the direction perpendicular to rotation axis. The non-equlibrium dynamics of superfluid is then determined by the friction forces at the boundaries. The mean free-flight time for electron-cluster scattering is (Paper I)

$$\tau_{eC}^{-1} = \frac{3\pi^3}{64}\langle n_p\rangle n_n \frac{c\delta_p}{(k_e\delta_p)^2} . \tag{8}$$

The electron quasiparticle lifetime due to the electron-electron scattering in an ultrarelativistic electron Fermi-liquid is

$$\tau_{ee} = \frac{8\pi^4\hbar^6}{m_e^{*3}\langle W\rangle(k_B T)^2} \simeq \frac{\pi}{2\alpha^2}\frac{\hbar}{\epsilon_{eF}}\left(\frac{\epsilon_{eF}}{k_B T}\right)^2 , \tag{9}$$

where $m_e^* = \hbar k_e/c$ is the electron effective mass and ϵ_{eF} is the electron Fermi energy, k_B is the Boltzmann constant, T is the temperature, $\alpha = e^2/\hbar c$ is the fine-structure constant, and we used $\langle W\rangle = (\pi/\hbar)V(q)^2$, where $V(q) \sim 4\pi e^2/k_e^2$ is the Fourier transform of the Coulomb potential. The $e - e$ scattering relaxation time weakly varies with the core density: for typical electron wavenumber value $k_e = 0.56$ fm^{-1} (see Paper I) one finds $\tau_{ee} = 8.2 \times 10^{-18} T_7^{-2}$ s, where $T_7 = T/10^7$ K. The electron-cluster scattering time varies in the range (1–500) $\times 10^{-15}$ s (Paper I). Thus, an increase of proton vortex number density by two to five orders of magnitude, depending on the core density, will lead to the *clumped regime* described above. It is evident that the hydrodynamic equations of Paper I are not valid in this regime.

The lattice constant of a triangular proton vortex lattice, d_p, is related to their number density as $\langle n_p\rangle = 2/(3)^{1/2}d_p^2$. Therefore, with increasing $\langle n_p\rangle$, the lattic constant will decrease until $d_p \sim \xi_p$, where ξ_p is the coherence length of the proton superconductor. In other words, the increase in the number density of proton vortices will obviously stop when the vortex cores touch each other, and the quasiparticles bound in the core merge in the continuum of the normal state. The required magnitude of the increase of proton vortex number with respect to the equilibrium ground state is of order $d_p^2/\xi_p^2 \sim 10^4$.

In the following discussion it will be assumed that the ground state vortex configuration is stable against any nonequilibrium disturbances.

3. SUPERFLUID ROTATION DYNAMICS WITH SPATIAL DEPENDENCE OF FRICTION

In this section we formulate a theory of superfluid rotation which includes spatial dependence of the mutual friction between the superfluid and the normal components. The theory is designed to describe the superfluid core rotation in neutron stars, therefore the dynamical equations will be written for vortex clusters—structures intrinsic to the neutron-proton superfluid mixture. However, as shown in Paper I, the resulting dynamical equations are formally identical to those for a single uncharged superfluid, the only difference being the definition of the effective neutral superfluid density and the mutual friction coefficients in the equation of motion of vortex clusters. Consequently, the results of this section are straightforwardly applicable to the single uncharged superfluids as

well. Our starting equations will be identical with the well-known general equations of dynamics of rotating superfluids, which have been widely discussed in the literature (see references in § 1). However, in order to be self-contained we will start below from first principles.

We will further restrict ourselves here to a system with a cylindrical geometry. The system is assumed to rotate around its symmetry axis, while the superfluid region is assumed to be enclosed between coaxial cylindrical boundaries with the inner radius R_i and the outer radius R_0. In model calculations the inner radius will correspond to the inner boundary of coexistence region of neutron-proton superfluid mixture and the outer radius will be identified with the crust-core boundary. Note that the sizes of the irrotational regions existing on the phase separation boundaries are of order of the intercluster spacing and can be neglected.

3.1. *The Basic Equations*

Equations governing the dynamics of the superfluid core rotation are

$$\text{curl } \boldsymbol{v}_s = \boldsymbol{v}_n n(\boldsymbol{r}, t) , \tag{10}$$

$$\rho_s^*[\boldsymbol{v}_s - \boldsymbol{v} \times \boldsymbol{v}_n] - \eta(r)(\boldsymbol{v} - \boldsymbol{v}_e) + \eta'(r)[\boldsymbol{v} - \boldsymbol{v}_e \times \boldsymbol{v}_n] = 0 , \tag{11}$$

$$\frac{\partial n(\boldsymbol{r}, t)}{\partial t} + \text{div } [n(\boldsymbol{r}, t)\boldsymbol{v}] = 0 , \tag{12}$$

where $\boldsymbol{v}_s$, $\boldsymbol{v}$, and $\boldsymbol{v}_e$ are the velocities of neutron superfluid, vortex clusters, and normal electron liquid, respectively, in the laboratory frame; ρ_s^* is the effective neutron superfluid density; $\boldsymbol{v}_n = \pi\hbar/m_n$ is the quantum of neutron vortex circulation; η and η' are the longitudinal and transverse viscous friction coefficients and $n(\boldsymbol{r}, t)$ is the local number density of vortex clusters.

In equation (10), which is the quantization of neutron superfluid velocity $\boldsymbol{v}_s$, an averaging procedure is carried out by replacing the summation over positions of discrete vortex clusters by their local mean number density, $n(\boldsymbol{r}, t)$.

Equation (11) gives the balance of the effective Magnus force and friction forces acting per unit length of a vortex cluster. The forces associated with the dynamical changes in the vortex shapes in the bulk of core are omitted, which is justified owing to the large tension of vortex cluster. Then, the frictional forces acting on the vortices at the boundaries can be absorbed in the second and the third terms of equation (11) (see Paper I). The viscous friction coefficients η and η' are found to be strongly position dependent. The variation lengthscale of these quantities is, however, much larger than the intercluster spacing and therefore the averaging procedure in equation (10) can be performed.

Equations (10)–(12) should be supplemented by the equation of motion of the normal component:

$$\frac{d}{dt} I_c \omega(t) = \mathscr{K}_{\text{int}}(t) + \mathscr{K}_{\text{ext}}(t) . \tag{13}$$

Here I_c and $\omega(t)$ are the moment of inertia and the angular velocity of the normal component, $\mathscr{K}_{\text{int}}(t)$ is the internal torque produced by the interaction of the superfluid and normal components, and $\mathscr{K}_{\text{ext}}(t)$ is the external braking torque acting on the normal component of the star.

The external torque is associated with the magnetosphere of the neutron star and is observed to change on timescales much larger than times of the irregularities of pulsar rotation. Therefore we assume the external braking torque, $\mathscr{K}_{\text{ext}}$, to be constant. The exact form of this torque is unimportant.

In the case of an axially symmetrical system equations (10)–(13) can be reduced to two coupled scalar equations for the angular velocities of the superfluid and normal components. Writing the vortex cluster velocity in the cylindrical coordinates (r, ϕ, z) as $\boldsymbol{v} = [\boldsymbol{v}_n \times \boldsymbol{e}_r]\omega r + \boldsymbol{e}_\varphi v_\varphi + \boldsymbol{e}_r v_r$, equations (10)–(12) give

$$v_r = \frac{\eta(r)\rho_s^* v_n}{\eta^2(r) + [\rho_s^* v_n - \eta'(r)]^2}[\omega_s(r, t) - \omega(t)]r , \tag{14}$$

$$v_\varphi = \frac{\rho_s^* v_n - \eta'(r)}{\eta(r)} v_r , \tag{15}$$

$$\frac{\partial}{\partial t} n(r, t) + \frac{1}{r}\frac{\partial}{\partial r} n(r, t) v_r r = 0 , \tag{16}$$

$$r\frac{\partial}{\partial r}\omega_s(r, t) + 2\omega_s(r, t) = v_n n(r, t) , \tag{17}$$

where $\omega_s = v_s/r$ is the local superfluid angular velocity. Integrating equation (16) over r and eliminating $n(r, t)$ from the last two equations, one finds

$$\frac{\partial}{\partial t}[\omega_s(r, t)r^2] = -v_r \frac{\partial}{\partial r}[\omega_s(r, t)r^2] . \tag{18}$$

Next substituting equation (14) in equation (18) the latter is transformed to the following form:

$$\frac{\partial}{\partial t}\Omega_s(r, t) = -a(r)\Omega_s(r, t)[\Omega_s(r, t) - q(r)\Omega(t)] - \frac{a(r)r}{2}[\Omega_s(r, t) - q(r)\Omega(t)]\left\{\frac{\partial}{\partial r}\Omega_s(r, t) - \frac{\Omega_s(r, t)}{q(r)}\frac{\partial q(r)}{\partial r}\right\} , \tag{19}$$

where reduced variables

$$\Omega_s(r, t) = \frac{\omega_s(r, t)}{\omega_s(r, 0)}, \qquad \Omega(t) = \frac{\omega(t)}{\omega(0)}, \qquad q(r) = \frac{\omega(0)}{\omega_s(r, 0)}, \tag{20}$$

are introduced. The quantity $q(r, 0)$ is the magnitude of disequilibrium between the normal and the superfluid components of the system at $t = 0$, (i.e., the onset of a macrojump). Under stationary conditions $q(r)$ deviates slightly from unity due to equilibrium departure between the rotation rates of superfluid and the normal component, when the system is subject to external decelerating torque. Along with $q(r)$ the quantity $\Delta(r) \equiv q(r) - 1$, which is the relative magnitude of the jump, will be used.

The function $a(r)$ in equation (19) is defined as

$$a(r) = \frac{2\omega(r, 0)}{q(r)} \frac{\rho_s^* v_n}{\eta(r)} \left\{1 + \left[\frac{\rho_s^* v_n - \eta'(r)}{\eta(r)}\right]^2\right\}^{-1}, \tag{21}$$

and contains microscopic parameters of the problem.

A general expression for the internal torque is

$$\mathcal{K}_{\text{int}} = \int [\boldsymbol{F}^{(fr)}(r) \times \boldsymbol{e}_r] r n(r, t) dV, \tag{22}$$

where $\boldsymbol{F}^{(fr)}(r)$ is the viscous friction force per unit length of a cluster, given by the second and the third terms of equation (11). Writing this force in components, we find

$$\begin{aligned} \mathcal{K}_{\text{int}}(t) &= -2\pi v_n \int \rho_s^* v_r n(r, t) l r^3 \, dr \\ &= -\frac{d}{dt} \omega(0) \int q(r)^{-1} \Omega_s(r, t) dI_s(r), \end{aligned} \tag{23}$$

where l is the length of the vortex cluster, R_i and R_0 are the inner and outer radii of the superfluid neutron-proton shell. Thus, equation (13) takes the form

$$\frac{d}{dt}\left[\Omega(t) + \int q(r)^{-1} \Omega_s(r, t) dp\right] = \gamma, \tag{24}$$

where additional reduced quantities

$$\gamma = \frac{\mathcal{K}_{\text{ext}}}{I_n \omega(0)}, \qquad dp = \frac{dI_s}{I_c} \tag{25}$$

are introduced.

Given the function $a(r)$ and the gross structure parameters of the neutron star, the system of coupled equations (19) and (24) determines the dynamics of rotation of the superfluid core.

3.2. *Dynamics of the Macrojump Relaxation*

In this section we find analytical solutions of the postjump relaxation problem where there is spatial dependence of the mutual friction. Solutions include all orders of the perturbation expansion with respect to the ratio $p_0 \equiv I_s/I_c$ of the superfluid moment of inertia to that of the normal component. In finding the result we will employ the following observational facts:

1. Measured relative magnitudes of pulsar macrojumps are no more than of order of 10^{-9}–10^{-6} and therefore we assume that $\delta\omega/\omega \ll 1$, where $\delta\omega = \omega(t) - \omega(0)$.

2. The external torque acting on the star *during* the relaxation process is effectively constant, i.e., we will assume γ in equation (24) to be time independent. Indeed, the characteristic times of external torque variations are of order the pulsar lifetime $\tau_0 \sim \omega/(2\dot{\omega}) \sim 10^3$–$10^9$ yr and are extremely large compared to the postjump relaxation timescales.

3. The ratio of moment of inertia of the superfluid involved in the postjump relaxation to the moment of inertia of the normal component, $p_0 \equiv I_s/I_c$, is small. A precise criterion of smallness of p_0 follows from the requirements for convergence of the power series expansion with respect to this parameter, and will be found below.

We note that the moment of inertia of the superfluid region involved in the postjump relaxations depends generally on the combination of two factors: (1) the superfluid gas profiles, and (2) the central density of the star and the stiffness of the equation of state, that regulate the size and moment of inertia of superfluid regions. Calculations of dynamical coupling times show that the integrated moment of inertia of the superfluid region *responsible for the postjump relaxations* is sufficiently small.

Now let us turn to the coupled equations (19) and (24). Considering small deviations from equilibrium, (see item 1), equation (19) can be linearized by substituting $\Omega_s(r, t) = 1 + \delta\omega_s(r, t)$, $\delta\omega_s(r, t) \ll 1$. The term associated with local spatial gradients, (the last term in braces of eq. [19]), can be dropped if the conditions $|(r/2)(\partial\, \delta\omega_s/\partial r)| \ll 1$ and $|(r/2)(\partial q/\partial r)| \ll 1$ are satisfied. The first condition can be roughly approximated as $(r/2)[\partial\, \delta\omega_s(r)/\partial r] \sim (r/\bar{r})[\delta\omega_s(\bar{r})] \ll 1$, where $\bar{r}$ is the characteristic variation length of function $\delta\omega_s(r)$. Due to smallness of $\delta\omega_s \sim \delta\omega$, it is a good approximation to drop the respective gradient term, provided $\bar{r}$ is a macroscopic length. To prove the second condition, note that $q(r) = [1 + \tau_d(r)/\tau_0 - \delta\omega(0)/\omega(0)]^{-1} \approx [1 - \tau_d(r)/\tau_0]$, where τ_d is the dynamical coupling

time defined by the formula (44) below, and we used the relation $\omega_s(0, r) - \omega(0) = [\tau_d/\tau_0]\omega(0) - \delta\omega(0)$, which specifies the initial state as discussed later (see eqs. [55] and [57]). Then $|(r/2)(\partial q/\partial r)| \approx |(r/2\tau_0)(\partial\tau_d/\partial r)|$, and since the ratio τ_d/τ_0 is typically of order 10^{-6}–10^{-3} and its variations are on macroscopic scales, this gradient term can be dropped as well. Note that generally the $q(r)$ function depends on the dynamical coupling model, and estimates here are based on the results of calculations for the superfluid core given in § 4.2.

After linearizing equation (19) and integrating equation (24) over time we get

$$\frac{\partial}{\partial t}\,\delta\omega_s(r, t) + a(r)\delta\omega_s(r, t) = -a(r)[1 - q\Omega(t)]\,, \tag{26}$$

$$\Omega(t) = 1 - p_0 \int_0^1 dy q(r)^{-1}\delta\omega_s - \gamma t\,, \tag{27}$$

where $dp \equiv p_0\,dy$, with initial conditions $\Omega(t) = 1$ and $\delta\omega_s(r, t) = 0$ at $t = 0$.

Substituting equation (26) into equation (27), we seek the solution of the resulting equation as a power series expansion of the small parameter $p_0 = I_s/I_c$:

$$\delta\omega_s = \sum_{k=0}^{\infty} p_0^k\,\delta\omega_s^{(k)}\,, \tag{28}$$

where the expansion coefficients $\delta\omega_s^{(k)}$ are determined from the equations

$$\frac{\partial}{\partial t}\,\delta\omega_s^{(0)} + a\,\delta\omega_s^{(0)} = -a(1 - q) - qa\gamma t\,, \tag{29}$$

$$\frac{\partial}{\partial t}\,\delta\omega_s^{(k)} + a\,\delta\omega_s^{(k)} = -a\int dy\,\delta\omega_s^{(k-1)}\,, \quad k = 1, 2, \ldots \tag{30}$$

In the hierarchy of coupled equations (29)–(30), each order correction is determined by the result found in the previous order of perturbation expansion. Solving successively equations (29) and (30), the zeroth-, first-, and second-order solutions are found to be

$$\delta\omega_s^{(0)} = \left(\Delta + q\,\frac{\gamma}{a}\right)(1 - e^{-at}) - q\gamma t \tag{31}$$

$$\delta\omega_s^{(1)} = \int dy_1\left(\Delta_1 + q_1\,\frac{\gamma}{a_1}\right)\left[\frac{a_1}{a - a_1}\,(1 - e^{-a_1 t}) + \frac{a}{a_1 - a}\,(1 - e^{-at})\right] - q\,\frac{\gamma}{a}\,(1 - e^{-at}) + q\gamma t\,, \tag{32}$$

$$\begin{aligned}\delta\omega_s^{(2)} = {} & \iint dy_2\,dy_1\left(\Delta_2 + q_2\,\frac{\gamma}{a_2}\right)\left\{\frac{a_1 a_2}{(a - a_1)(a - a_2)}\,(1 - e^{-at}) + \frac{aa_2}{(a_1 - a)(a_1 - a_2)}\,(1 - e^{-a_1 t}) + \frac{aa_1}{(a_2 - a)(a_2 - a_1)}\,(1 - e^{-a_2 t})\right\} \\ & + \int dy_2\,q_2\,\frac{\gamma}{a_2}\left[\frac{a}{a - a_2}\,(1 - e^{-a_2 t}) + \frac{a_2}{a_2 - a}\,(1 - e^{-at})\right] + q\,\frac{\gamma}{a}\,(1 - e^{-at}) - q\gamma t\,.\end{aligned} \tag{33}$$

By inspection, the kth order correction has a general form

$$\begin{aligned}\delta\omega_s^{(k)} = {} & \int dy_k \ldots dy_1\Delta_k \sum_{i=0}^{k}\left[\prod_{\substack{l=0\\ i\neq l}}^{k}\frac{a_l}{(a_i - a_l)}\right](1 - e^{-a_i t}) \\ & + (-1)^k q_k\,\frac{\gamma}{a_k}\sum_{n=1}^{k}\int dy_n \ldots dy_1 \sum_{i=0}^{n}\left[\prod_{\substack{l=0\\ i\neq l}}^{k}\frac{a_l}{(a_i - a_l)}\right](1 - e^{-a_i t}) + (-1)^k\left[\frac{q\gamma}{a}\,(1 - e^{-at}) - q\gamma t\right].\end{aligned} \tag{34}$$

Here $a_k \equiv a(y_k)$, $q_k \equiv q(y_k)$, and $\Delta_k \equiv \Delta(y_k)$. Substituting solutions (31)–(33) into the expansion (28) we find the net deviation of the superfluid angular velocity:

$$\begin{aligned}\delta\omega_s = {} & -q\,\frac{\gamma}{1 + p_0}\,t + \left[\Delta + q\,\frac{\gamma}{(1 + p_0)a}\right](1 - e^{-at}) + p_0\int dy_1\left[\Delta_1 + q_1\,\frac{\gamma}{(1 + p_0)a_1}\right] \\ & \times\left\{\frac{a}{a_1 - a}\,(1 - e^{-a_1 t}) + \frac{a_1}{a - a_1}\,(1 - e^{-at})\right\} + p_0^2\iint dy_1\,dy_2\left[\Delta_2 + q_2\,\frac{\gamma}{(1 + p_0)a_1}\right] \\ & \times\left\{\frac{a_1 a_2}{(a - a_1)(a - a_2)}\,(1 - e^{-at}) + \frac{aa_2}{(a_1 - a)(a_1 - a_2)}\,(1 - e^{-a_1 t}) + \frac{aa_1}{(a_2 - a)(a_2 - a_1)}\,(1 - e^{-a_2 t})\right\} + \mathcal{O}(p_0^3)\,.\end{aligned} \tag{35}$$

Substituting this result in the equation (27) we get the normalized angular velocity

$$\Omega(t) = 1 - \gamma t\left(1 - \frac{p_0}{1+p_0}\right) - p_0 \int dy\left[\Delta + \frac{\gamma}{(1+p_0)a}\right](1 - e^{-at}) + p_0^2 \iint dy\, dy_1\left[\Delta_1 + \frac{\gamma}{(1+p_0)a_1}\right]$$
$$\times \left\{\frac{a}{a_1 - a}(1 - e^{-a_1 t}) + \frac{a_1}{a - a_1}(1 - e^{-at})\right\} + p_0^3 \iiint dy\, dy_1\, dy_2\left[\Delta_2 + \frac{\gamma}{(1+p_0)a_2}\right]$$
$$\times \left\{\frac{a_1 a_2}{(a-a_1)(a-a_2)}(1 - e^{-at}) + \frac{aa_2}{(a_1 - a)(a_1 - a_2)}(1 - e^{-a_1 t}) + \frac{aa_1}{(a_2 - a)(a_2 - a_1)}(1 - e^{-a_2 t})\right\} + \mathcal{O}(p_0^4)\,. \tag{36}$$

Here, for the sake of simplicity, a replacement $\Delta_k/q_k \approx \Delta_k$, which neglects terms of order of Δ_k^2 is made. This result may be further modified by combining together the terms containing identical exponential factors. Then equation (36) takes the form

$$\Omega(t) = 1 - \frac{\gamma}{1+p_0}\,t - p_0 \int dy\left[\Delta + \frac{\gamma}{(1+p_0)a}\right](1 - e^{-at})\{1 + p_0 \mathcal{I}(y) + p_0^2 \mathcal{I}^2(y) + \mathcal{O}[p_0^3 \mathcal{I}^3(y)]\}$$
$$- p_0 \int dy_1\left[\Delta_1 + \frac{\gamma}{(1+p_0)a_1}\right](1 - e^{-a_1 t})\{p_0 \mathcal{I}(y_1) + p_0^2 \mathcal{I}^2(y_1) + \mathcal{O}[p_0^3 \mathcal{I}^3(y_1)]\}$$
$$- p_0 \int dy_2\left[\Delta_2 + \frac{\gamma}{(1+p_0)a_2}\right](1 - e^{-a_2 t})\{p_0^2 \mathcal{I}^2(y_2) + p_0^3 \mathcal{I}^3(y_2) + \mathcal{O}[p_0^4 \mathcal{I}^4(y_2)]\} - \cdots, \tag{37}$$

where

$$\mathcal{I}(y) = \int_0^1 dy_1 \frac{a_1(y_1)}{a(y) - a_1(y_1)}\,. \tag{38}$$

Summing up the infinite series in equation (37) with respect to the parameter $p_0 \mathcal{I}(y)$, one finds

$$\Omega(t) = 1 - \frac{\gamma}{1+p_0}\,t - p_0 \int dy\left[\Delta + \frac{\gamma}{(1+p_0)a}\right](1 - e^{-at})\frac{1}{[1 - p_0 \mathcal{I}(y)]^2}\,. \tag{39}$$

Finally going over from the reduced to the initial variables and introducing notations $\tau_0 = (1+p_0)/\gamma$ and $\tau_d = a^{-1}$ we get the angular frequency of the normal component and its first derivative

$$\omega(t) = \omega(0)\left\{1 - \frac{t}{\tau_0} - \frac{1}{I_c}\int d\tau_d\left[\frac{dI_s(\tau_d)}{d\tau_d}\right]\left(\Delta + \frac{\tau_d}{\tau_0}\right)(1 - e^{-t/\tau_d})\frac{1}{[1 - (I_s/I_c)\mathcal{I}(\tau_d)]^2}\right\}, \tag{40}$$

$$\dot{\omega}(t) = \omega(0)\left\{-\frac{1}{\tau_0} - \frac{1}{I_c}\int d\tau_d\left[\frac{dI_s(\tau_d)}{d\tau_d}\right]\left(\Delta + \frac{\tau_d}{\tau_0}\right)\frac{e^{-t/\tau_d}}{\tau_d}\frac{1}{[1 - (I_s/I_c)\mathcal{I}(\tau_d)]^2}\right\}. \tag{41}$$

The conditions determining the limits of validity of our result follow from the requirements of the convergence of the infinite power series that were summed in finding the equations (35) and (39). These conditions are

$$p_0 \equiv \frac{I_s}{I_c} < 1\,, \qquad \frac{I_s}{I_c}\mathcal{I}(\tau_d) < 1\,, \tag{42}$$

where

$$\mathcal{I}(\tau_d) = \int_{\tau(R_i)}^{\tau(R_0)} d\tau_{d1}\left[\frac{dI_s(\tau_{d1})}{d\tau_{d1}}\right]\frac{\tau_d}{\tau_{d1} - \tau_d}\,, \tag{43}$$

and $\tau_d(R_i)$ and $\tau_d(R_0)$ are the values at the inner and outer boundaries of the superfluid shell.

According to equations (40) and (41), the relaxation of the jump in the rotation frequency of the normal component of the star is characterized by an exponential decay with timescale τ_d. This timescale is generally a strongly varying function of the position in the star. The exponential relaxation is weighted by the factor $[1 - (I_s/I_c)\mathcal{I}(\tau_d)]^{-2}$, which is accounting for the correlations between the superfluid shells with different dynamical coupling times. The dynamical coupling timescales are defined as (see eq. [21])

$$\tau_d = \frac{q(r)}{2\omega(0)}\frac{\eta}{\rho_s^* v_n}\left[1 + \left(\frac{\rho_s^* v_n - \eta'}{\eta}\right)^2\right]. \tag{44}$$

For a given region with a fixed effective neutron superfluid density ρ_s^*, the dynamical coupling time is uniquely determined by the viscous friction coefficients η, η', and the magnitude of disequilibrium, given by the function $q(r)$. Quite generally the viscous friction transverse to the direction of vortex motion is much smaller than the longitudinal friction, i.e., $\eta' \ll \eta$, and may be further neglected.

The dependence of τ_d on η is not trivial. The dynamical coupling timescale acquires large values in two opposite limits, $\eta \gg \rho_s^* v_n$ and $\eta \ll \rho_s^* v_n$. It is minimal when $\eta = \rho_s^* v_n$, with minimum value $\tau_d = q(r)/\omega(0)$. In the *strong coupling limit* between the normal

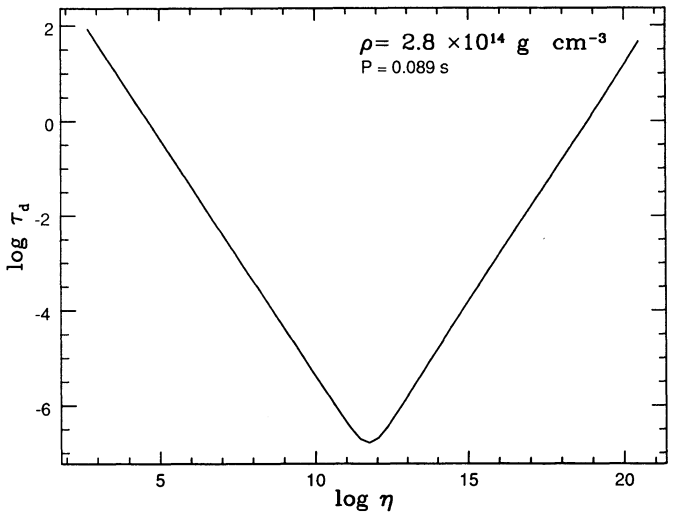

FIG. 2.—Dependence of the dynamical coupling time on the viscous friction coefficient for superfluid density $\rho_s^* = 2.8 \times 10^{14}$ g cm^{-3} and the spin period of the Vela pulsar $P = 0.089$ s. The left branch of the curve corresponds to the weak coupling limit between vortices and the normal component, which produces macroscopic (observable) timescales, while the right branch to the strong coupling limit. The minimal coupling timescale is a fraction of a second.

component and the vortex clusters, i.e., $\eta \gg \rho_s^* v_n$, the vortex clusters are dragged by the normal matter in the azimuthal direction and have small radial velocity component due to the high viscous friction. This may be observed by considering the strong coupling limit in the equations (14) and (15), from which follows $v_\phi \to \omega r$ and $v_r \to 0$.

In the *weak coupling limit*, $\eta \ll \rho_s^* v_n$, the vortex clusters flow with the superfluid, again with a small radial component owing to weak friction; in other words, $v_\phi \to v_n$ and $v_r \to 0$. Since the dynamical relaxation proceeds by the radial expansion or compression of the neutron vortex lattice, in both cases the relaxation times appear to be long. The general $\tau_d(\eta)$ dependence for the Vela pulsar, $P = 0.089$ s, is given in Figure 2.

While the previous couplings models of Feibelman (1971) and Sauls, Stein, & Serene (1982) correspond to the weak coupling limit producing observable relaxation timescales (left branch of Fig. 2), and the model of Alpar et al. (1984b) implying short dynamical coupling times is an intermediate coupling model, the present model is based on the strong coupling limit between vortex clusters and normal component (right branch of Fig. 2).

4. THE SHELL MODEL AND COMPARISON WITH THE POSTJUMP DATA

The postjump relaxations of pulsars are commonly fitted by assuming a sequence of exponential decays plus a long term linear decay on time independent scales. The long-term linear decay can be simply understood as an exponential decay with a time constant much larger than the observation timescale. The discreteness of time constants implies that distinct superfluid shells are responding to the jump independently. In the remainder of this paper the continuous model of previous sections will be simplified to a discrete shell model, and the possibilities of understanding of postjump data in terms of the shell model for the superfluid core will be explored.[3]

4.1. *Postjump Relaxation in the Shell Model*

Next we assume that the bulk of the superfluid shell may be divided into several distinct superfluid regions that respond to the jump independently. Neglecting correlations implies that one can set $[1 - (I_s/I_c)\mathcal{I}(\tau_d)]^2 = 1$ in the general result (40). Replacing the remaining integration over the entire superfluid region by a summation over a finite number of superfluid shells we get

$$\nu(t) = \nu_0 - \frac{\nu_0}{\tau_0} t - \sum_i \frac{I_{si}}{I_c} \left(\frac{\nu_0}{\tau_0} \tau_i - \Delta\nu_{si} \right) (1 - e^{-t/\tau_i}) , \tag{45}$$

$$\dot{\nu}(t) = -\frac{\nu_0}{\tau_0} - \sum_i \frac{I_{si}}{I_c} \left(\frac{\nu_0}{\tau_0} \tau_i - \Delta\nu_{si} \right) \frac{e^{-t/\tau_i}}{\tau_i} , \tag{46}$$

where notations $\nu(t) = \omega(t)/2\pi$, $\nu(0) \equiv \nu_0$, $\nu_s(t) = \omega_s(t)/2\pi$ are introduced and the substitutions $\Delta_i = q_i - 1 = -\Delta\nu_{si}/\nu_0$, $\Delta\nu_{si} = \nu_{si}(0) - \nu_0$ are made. The similarity of these equations to that of the two-component model of Baym et al. (1969) is obvious.

Below we will restrict the discussion to a three-shell model, where the postjump response is described by short, (*s*), intermediate, (*i*), and long, (*l*), decay time constant. This choice is largely motivated by the analysis of postjump data by Cordes et al. (1988) which

[3] We note that a multiplicity of combinations of relaxation time constant can fit the postjump behavior as well. See, e.g., the analysis of the postjump relaxations of the Vela pulsar by Cordes et al. (1988) and Alpar et al. (1993).

will be discussed later. Now we will make an assumption that the reduced moment of inertia of the short and intermediate shells, $p_s = I_{ss}/I_c$ and $p_i = I_{si}/I_c$ satisfy the condition $p_s \ll 1$, $p_i \ll 1$, which will be proven á posteriori from the comparison of the model calculations with the postjump data. However the moment of inertia of the l shell can be a considerable fraction of the moment of inertia of the crust. Under these circumstances the independent shell approximation given by equations (45) and (46) should be modified. We will show next that the terms describing the coupling of the long-term response shell to the s and i shells are of order of $p_l p_j$, $j = s, i$ and can be therefore ignored. The resulting equations are identical with equations (45) and (46) for the s, i shell and are slightly different for the l shell.

Let us go back to equations (26)–(27). In the three-shell case they can be rewritten in the following form:

$$\frac{\partial}{\partial t}\,\delta\omega_{sl} + a_l(1 + p_l)\delta\omega_{sl} = -a_l(1 - q_l) - q_l a_l \gamma t\,, \tag{47}$$

$$\frac{\partial}{\partial t}\,\delta\omega_{sj} + a\,\delta\omega_{sj} = -a_j(1 - q_j) - a_j q_j \gamma t - a_j p_l\,\delta\omega_{sl} \quad j = s, i\,. \tag{48}$$

$$\Omega(t) = 1 - \sum_j p_j q_j^{-1}\delta\omega_j - p_l q_l^{-1}\delta\omega_l - \gamma t\,. \tag{49}$$

Solving successively equations (48) and (47) and substituting the results in equation (49), one finds the normalized spin frequency

$$\Omega = 1 - \frac{\gamma}{1 + p_l}\,t - p_j\left[\Delta_j + \frac{\gamma}{(1 + p_l)a_j}\right](1 - e^{-a_j t}) - p_l\left[\frac{\Delta_l}{1 + p_l} + \frac{\gamma}{(1 + p_l)^2 a_l}\right](1 - e^{-a_l(1 + p_l)t})$$
$$- p_l p_j\left[\frac{\Delta_l}{1 + p_l} + \frac{\gamma}{(1 + p_l)^2 a_l}\right]\left\{\frac{a_j(1 - e^{-a_l(1 + p_l)t}) - a_l(1 + p_l)(1 - e^{-a_j t})}{a_j - (1 + p_l)a_l}\right\}. \tag{50}$$

Introducing notation $\tau_k^{-1} = (1 + p_k)a_k$, where $k = s, i, l$, we get

$$v(t) = v_0 - \frac{v_0}{\tau_0}\,t - \sum_{k=1}^{3}\frac{p_k}{1 + p_k}\left[\frac{v_0}{\tau_0}\,\tau_k(1 + p_k) - \Delta v_{sk}\right](1 - e^{-t/\tau_k}) + \sum_{j=1}^{2}\frac{p_l p_j}{1 + p_l}\left[\frac{v_0}{\tau_0}\,\tau_l(1 + p_l) - \Delta v_{sl}\right]\frac{\tau_l(1 - e^{-t/\tau_l}) - \tau_j(1 - e^{-t/\tau_j})}{\tau_l - \tau_j}\,, \tag{51}$$

$$\dot{v}(t) = -\frac{v_0}{\tau_0} - \sum_{k=1}^{3}\frac{p_k}{1 + p_k}\left[\frac{v_0}{\tau_0}\,\tau_k(1 + p_k) - \Delta v_{sk}\right]\frac{e^{-t/\tau_k}}{\tau_k} + \sum_{j=1}^{2}\frac{p_l p_j}{1 + p_l}\left[\frac{v_0}{\tau_0}\,\tau_l(1 + p_l) - \Delta v_{sl}\right]\frac{e^{-t/\tau_l} - e^{-t/\tau_j}}{\tau_l - \tau_j}\,. \tag{52}$$

The terms $\propto p_l p_j$ can be dropped since $p_j \ll 1$ and, as estimated below, $p_l < 0.5$. Then equations (51) and (52) are essentially identical with equations (45) and (46) with the exception that the dynamical coupling time for long-term response and the magnitude of the initial disequilibrium are reduced by a factor $1 + p_l$. In this approximation the expression for the superfluid spin frequency is the same for all three superfluid shells and has the form

$$v_{sk}(t) = v(0) - \frac{v_0}{\tau_0}\,t + \frac{1}{1 + p_k}\left[\frac{v_0}{\tau_0}\,\tau_k(1 + p_k) - \Delta v_{sk}\right](1 - e^{-t/\tau_k}), \quad k = s, i, l\,. \tag{53}$$

It can be seen from equations (51) and (52), that the postjump behavior of $v(t)$ and $\dot{v}(t)$ depends in an essential way on the amplitude of the jump in each shell which, in its turn, depends on the prejump spin frequency of the given shell attained in the interjump epoch. Therefore let us look for the respective equilibrium state solutions.

Differentiating equation (53) with respect to time and taking the limit $t/\tau_j \to \infty$ in the resulting equation and in equation (52) one finds the equilibrium state solution, ($\Delta v_{sk} = 0$),

$$\dot{v}(\infty) = \dot{v}_s(\infty) = -\frac{v_0}{\tau_0}\,, \tag{54}$$

i.e., the equilibrium spin-down rates are the same for the normal and superfluid components. Further, using equations (51) and (53),

$$v_{sk}(\infty) - v(\infty) = \frac{v_0}{\tau_0}\,\tau_k(1 + p_k)\,, \tag{55}$$

i.e., the equilibrium spin frequency of the superfluid component is larger than that of the normal component by a positive number, $\Delta v_{sj}(\infty) \geq 0$, and depending on whether it is larger or smaller than $v_0\,\tau_k(1 + p_k)/\tau_0$, the normal component spins-up or spins-down.

However, complete equilibrium may not be achieved in a number of shells for several reasons. One reason is that considerable pinning forces can act on the vortex clusters at the boundaries. The boundary pinning is caused by the interaction of the vortex clusters with the nonregularities of the crust core boundary interface. This process is analogous to the boundary pinning in rotating terrestrial superfluids like ^{4}He and ^{3}He, and will be discussed in detail separately.

Second, a nonequilibrium state can arise, even in the absence of pinning, due to fluctuations in the number density of vortex lines. In the regions with large relaxation timescales the equilibrium departure of the superfluid spin frequency from that of the normal component can be much larger than the magnitude of the jump, therefore small fluctuations superposed on this state can essentially change the initial conditions for a postjump relaxation process.

The superfluid spin frequency departure *before* the jump can be written as

$$\Delta\nu_{sj}(0^-) = \frac{\nu_0}{\tau_0}\tau_j(1+p_j) + \Delta\nu_{sj}^{(ex)}\,, \tag{56}$$

where $\Delta\nu_s^{(ex)}$ is the prejump deviation of $\Delta\nu_s$ from its value in the equilibrium. Then the initial conditions in the equations describing the postjump response are found by subtracting the jump in the spin frequency of the crust, $\Delta\nu$, from equation (56)

$$\Delta\nu_{sj}(0^+) = \frac{\nu_0}{\tau_0}\tau_j(1+p_j) + \Delta\nu_{sj}^{(ex)} - \Delta\nu\,. \tag{57}$$

According to the prejump states the superfluid shells can be classified as follows:

1. $\Delta\nu_{sj}^{(ex)} < \Delta\nu$. The prefactor (amplitude) of the exponential functions in equation (52) is negative and the j shell causes a decrease of $\dot\nu$ after a macrojump, with an effective amplitude shifted with respect to the observed jump in the spin rate of the crust by $\Delta\nu_{sj}^{(ex)}$. Note that the relevant timescale for the relaxation process is the dynamical coupling timescale of that particular shell. Shells with such initial conditions will be called *relaxation shells.*

2. $\Delta\nu_{sj}^{(ex)} > \Delta\nu$. In this case the amplitude of the exponential function is positive and the j shell causes an increase of $\dot\nu$ after a macrojump. These shells will be called *rise shells.* This case will be considered in details in § 5.

3. In the special case $\Delta\nu_{sj}^{(ex)} = 0$, the shell is in a quasi-equilibrium spin-down state *before the jump* and the effective magnitude of the jump in the shell is equal to the observed magnitude of the macrojump in the spin rate of the crust. This is a particular case of a relaxation shell.

4. Finally, in the special case $\Delta\nu_{sj}^{(ex)} = \Delta\nu$, the shell is in quasi-equilibrium *after the jump* and therefore does not respond to the macrojump. Shells with such a particular initial condition, or the shells where the pinning is effective and they do not respond to the jump will be called *passive shells.*

In the shells where the free flow regime is realized in the interjump epoch, and therefore the equilibrium is achieved, initial conditions correspond to case 3. Those shells, where the equilibrium state is not attained or boundary pinning is effective the cases 1, 2, and 4 are possible.[4]

4.2. *Model Calculations and Comparison with Postjump Data from the Vela Pulsar (0833−45)*

The postjump relaxation from the Vela pulsar provide a suitable reference for quantitative modeling of postjump relaxation processes. We refer to Alpar et al. (1993) for a recent discussion of these data in terms of vortex creep model in the crust. Here we model the first six postjump relaxations of Vela pulsar relying on the work by Cordes et al. (1988). Analysis of subsequent glitches (7–11) is deferred to another paper. In the next section, we will discuss the implications of the present dynamical model for other pulsars.

The model equation applied in the analysis by Cordes et al. (1988) of the postjump behavior of the spin down rate of the Vela pulsar reads

$$\dot\nu(t) = \dot\nu_0 + \ddot\nu_0(t-t_0) + \sum_j \{[\dot\nu_{sj}\,e^{-(t-T_j)/\tau_{sj}} + \dot\nu_{ij}\,e^{-(t-T_j)/\tau_{si}} + \dot\nu_l + \ddot\nu_{lj}(t-T_j)]\theta(t-T_j)\theta(T_{j+1}-t)\}\,, \tag{58}$$

where t_0 is the reference epoch, $\dot\nu_0$ and $\ddot\nu_0$ are the spin-down rate and its derivative evaluated at the epoch t_0 in the absence of a jump, $\theta(t)$ is the step function, T_j is the time of the first observation after the jump occurred, T_{j+1} is the epoch of the next jump. Within this model the postjump response is described by short and intermediate exponential decays with time constants τ_s and τ_i, going over to a long linear decay with a time constant τ_l.

The long term decay constant is found to be much larger than the postjump observation times. Therefore in the respective term of equation (52), the exponential function can be expanded in a Taylor series with respect to t/τ_l keeping only the linear term. Further, substituting the initial condition (57) in the equation (52), we get

$$\dot\nu(t) = -\frac{\nu_0}{\tau_0}\left\{1 + \frac{I_{ss}}{I_c+I_{ss}}\frac{\Delta\nu}{\nu_0}\frac{\tau_0}{\tau_s}\left[1-\frac{\Delta\nu_{ss}^{(ex)}}{\Delta\nu}\right]e^{-t/\tau_s} + \frac{I_{si}}{I_c+I_{si}}\frac{\Delta\nu}{\nu_0}\frac{\tau_0}{\tau_i}\left[1-\frac{\Delta\nu_{si}^{(ex)}}{\Delta\nu}\right]e^{-t/\tau_i} + \frac{I_{sl}}{I_c+I_{sl}}\frac{\Delta\nu}{\nu_0}\frac{\tau_0}{\tau_l}\left[1-\frac{\Delta\nu_{sl}^{(ex)}}{\Delta\nu}\right]\left(1-\frac{t}{\tau_l}\right)\right\}. \tag{59}$$

In modelling the postjump behavior, the following constraints will be imposed:

1. In the relaxation shells responsible for the short, intermediate, and long postjump relaxations, it is assumed that $\Delta\nu_s^{(ex)} = 0$, i.e., these shells are assumed to be in an equilibrium spin down state before the jump. For the relaxation shell producing the long-term linear response the equilibrium spin-down state cannot be achieved because the respective dynamical coupling times are found to be larger than the interjump period. Indeed, the equilibrium superfluid spin frequency departure for an l-shell with e.g., $\tau_l \sim 10^3$ days is $[\Delta\nu_{sl}/\nu_0] = [\tau_l/\tau_0] \sim 10^{-4}$, ($\tau_0 \approx 2\times 10^4$ yr for the Vela pulsar). Therefore the magnitude of disequilibrium introduced by a jump, $\Delta\nu/\nu_0 \sim 10^{-6}$ is about 1% of the equilibrium departure and can be neglected. (Note however that small fluctuations superposed on the equilibrium state can essentially affect the initial conditions.)

2. The shells with dynamical timescales not revealed in the postjump analysis are assumed to be passive. In other words, it is assumed that either the superfluid component before the jump has a spin frequency excess of order of magnitude of the subsequent

[4] Note that, obviously, the equilibrium spin-down state can be achieved in the free flow regime only when the relaxation time for the given shell is smaller than the interjump period. Therefore the regions with $\tau_d > 10^3$ days for example in the Vela pulsar, do not achieve their equilibrium deceleration state.

jump, or the clusters are pinned to the crust-core boundary and consequently are not involved in the postjump response. Since the first case seems to be a very restrictive one, the pinned regime must be necessarily invoked.

Adopting these constraints equation (59) becomes

$$\dot{\nu}(t) = -\frac{\nu_0}{\tau_0} - \frac{I_{ss}}{I_c}\frac{\Delta\nu}{\tau_s}\, e^{-t/\tau_s} - \frac{I_{si}}{I_c}\frac{\Delta\nu}{\tau_i}\, e^{-t/\tau_i} - \frac{I_{sl}}{I_c + I_{sl}}\frac{\Delta\nu}{\tau_l}\left(1 - \frac{t}{\tau_l}\right). \tag{60}$$

Now we can use the fitting formula given by Cordes et al. (1988). Combining equations (58) and (60) one finds

$$\tau_l = \frac{|\dot{\nu}_0 + \dot{\nu}_l| - (\nu_0/\tau_0)}{\ddot{\nu}_0 + \ddot{\nu}_l}, \tag{61}$$

$$\frac{I_{sl}}{I_c + I_{sl}} = \frac{(\dot{\nu}_0 + \dot{\nu}_l)\tau_l}{\Delta\nu}, \tag{62}$$

$$\frac{I_{ss}}{I_c} = \frac{|\dot{\nu}_s|}{\Delta\nu}\tau_s, \tag{63}$$

$$\frac{I_{si}}{I_c} = \frac{|\dot{\nu}_i|}{\Delta\nu}\tau_i. \tag{64}$$

On the right-hand side of equations (61)–(64) appear quantities which were determined by Cordes et al. from their observational study of the first six postjump relaxations of the Vela pulsar. In Table 1 we reproduce their values for τ_s and τ_i and give calculated parameters on the left-hand side of equations (61)–(64). The range of the long term time constant is $430 \leq \tau_l \leq 1300$ days for different events, while the reduced moment of inertia is in the range $0.1 \leq p_l \leq 0.5$. The reduced moment of inertia of the short and the intermediate shells are two and one orders of magnitude smaller respectively.

Now we turn to the problem of identification of superfluid shells that can be responsible for the postjump relaxation processes. The short, intermediate, and long relaxation shells are characterized by two parameters—the time constant and the moment of inertia. Therefore, we have to find appropriate pairs of these parameters describing the short, intermediate, and long stages of postjump response for each postjump event. We use a neutron star model based on the equation of state of Wiringa, Fisks, & Fabrocini (1988) and we choose a star with mass $M = 1.4\ M_\odot$, which has a radius $R = 10.13$ km and total moment of inertia $I = 1.156 \times 10^{45}$. The microscopic proton superconductor parameters are from Baldo et al. (1992) (see Table 1 and 2 of Paper I). The inner radius of the superfluid neutron-proton shell is $R_i \simeq 5$ km, and corresponds to the matter densities $\rho_i \simeq 9.8 \times 10^{14}$ at which the proton superconducting gap vanishes. The estimate of the inner boundary R_i involves uncertainties due to difficulty of calculations of the proton superconductor parameters in the high-density regime, (see Baldo et al. 1992 and Wambach, Ainsworth, & Pines 1991). The moment of inertia in the shell $0 \leq r \leq R_i$ is $I[0, R_i] = 6.3 \times 10^{43}$ g cm^2, where r is the inner radius of the star. The outer radius of the superfluid neutron-proton shell is $R_0 = 9.64$ km, and corresponds to the density $\rho_0 = 1.68 \times 10^{14}$ g cm^{-3}, which is the density of the phase transition to the uniform liquid according to the result due to Lorenz, Ravenhall, & Pethick (1993). The moment of inertia enclosed in the shell $R_i \leq r \leq R_0$ is $I[R_i, R_0] = 9.85 \times 10^{44}$ g cm^2, while the original crust, (the shell $R_0 \leq r \leq R$) has moment of inertia $I[R_0, R] = 1.956 \times 10^{43}$ g cm^2. We will assume that the inner core shell $0 \leq r \leq R_i$, where the proton superconductivity vanishes, is rigidly rotating with the crust. Thus, the effective moment of inertia of the crust is $I_c = I[0, R_i] + I[R_0, R] = 8.3 \times 10^{43}$ g cm^2. Present calculations are based on the general relativistic neutron star models constructed by Weber (1992).

In Table 2, the density, the reduced moment of inertia, and the coupling time profiles in the superfluid neutron-proton shell are given. The dependence of coupling times on the reduced moment of inertia is continuous. We evaluate the shell model by appropriate averaging. In identifying the active regions one can start with the given observed time constant, find the respective value of p_s, and then choose a region with inferred value of Δp_s in the vicinty of this value in such a way that the mean value of τ_j over this region will be that given initially by the fit. In Table 3 the locations of relaxation shells for each postjump event, found by means of this procedure, are given. The remaining parameters of these shells can be read off from Table 2.

In Figure 3, we show the relaxation (shaded regions) and passive shells in each postjump relaxation process. From that figure it is evident that the relaxation shells are changing their location for different events. The fraction corresponding to the l shell is found to be large. According to equation (55) the large time constants of this shell imply that roughly 1% fluctuations superposed on the

TABLE 1

PARAMETER VALUES OF SUPERFLUID SHELLS INVOLVED IN THE POSTJUMP RELAXATIONS

Postjump	τ_s (days)	I_{ss}/I_c ($\times 10^{-3}$)	τ_i (days)	I_{si}/I_c ($\times 10^{-3}$)	τ_l (days)	I_{sl}/I_c
1	10.0	1.98	120.0	17.8	1091.9	0.22
2	4.0	1.58	94.00	13.1	740.2	0.181
3	4.0	0.44	35.00	3.53	877.3	0.517
4	6.0	2.41	75.00	11.3	1296.1	0.416
5	6.0	0.81	14.00	1.89	494.62	0.43
6	3.0	2.48	21.50	5.5	433.0	0.108

TABLE 2

INTERNAL STRUCTURE AND DYNAMICAL COUPLING TIMES IN THE SUPERFLUID CORE OF A $M = 1.4\ M_\odot$ MASS STAR

r (km)	p_s	$\rho(\times 10^{14}$ g cm$^{-3})$	τ_d(days)
8.59.....	0.297	5.638	1.24E+04
8.90.....	0.199	4.928	1.12E+04
9.02.....	0.161	4.628	9.56E+03
9.06.....	0.149	4.524	8.26E+03
9.08.....	0.141	4.439	7.12E+03
9.12.....	0.129	4.320	5.65E+03
9.15.....	0.121	4.223	4.71E+03
9.17.....	0.112	4.123	4.14E+03
9.20.....	0.104	4.016	3.81E+03
9.22.....	0.099	3.941	3.51E+03
9.25.....	0.091	3.821	2.86E+03
9.27.....	0.085	3.736	2.36E+03
9.28.....	0.080	3.649	1.88E+03
9.31.....	0.072	3.514	1.28E+03
9.33.....	0.067	3.418	9.54E+02
9.35.....	0.062	3.320	6.83E+02
9.37.....	0.058	3.221	4.69E+02
9.38.....	0.053	3.118	3.05E+02
9.40.....	0.048	3.018	1.91E+02
9.42.....	0.044	2.921	1.20E+02
9.44.....	0.040	2.827	7.56E+01
9.46.....	0.035	2.735	4.62E+01
9.47.....	0.033	2.684	3.44E+01
9.48.....	0.029	2.592	1.97E+01
9.50.....	0.025	2.498	1.05E+01
9.52.....	0.021	2.405	5.26E+00
9.53.....	0.019	2.358	3.60E+00
9.56.....	0.014	2.193	7.66E−01
9.57.....	0.010	2.094	2.54E−01
9.59.....	0.007	1.997	6.97E−02
9.62.....	0.003	1.830	3.85E−03
9.64.....	0.000	1.682	3.76E−04

NOTES.—Table 2 gives the internal structure of the superfluid neutron-proton shell of a $M = 1.4\ M_\odot$ constructed using the equation of state of Wiringa et al. 1988. The proton superconductor parameters are taken from Baldo et al. 1992. Here r is the internal radius, ρ and τ_d are the corresponding density and coupling times, and $p_s = [I_s(R_0) - I_s(r)]/I$ is the reduced moment of inertia of the superfluid shell calculated from the crust core boundary $r = R_0$.

equilibrium solution can block out the postjump response, i.e., can make the shell passive. The fraction of the i and especially the s-shells are typically much smaller, which implies much more effective pinning at the boundaries, than in the l shell.

We offer two arguments in favor of the occurrence of pinning. First, a purely geometrical argument can cause stronger pinning in the s and i shells, if we take into account the real spherical geometry of the star. Indeed, the l, i, and s shells are located at successively larger distances from the rotation axis of the star. Provided pinning forces at the crust-core interface are similar, regardless of the cylindrical radius of the cluster, the effect of shortening of vortex cluster as one moves from the deep interior to the crust boundary can be a reason for the pinning force *per unit length* to increase. Because the locations of active regions are changing from event to event, it seems that there are no *preferred* places of pinning, rather they appear to be random. Second, the equilibrium spin frequency

TABLE 3

LOCATIONS OF RELAXATION SHELLS IN THE SUPERFLUID CORE FOR A $M = 1.4\ M_\odot$ NEUTRON STAR WITH THE SPIN FREQUENCY OF THE VELA PULSAR

Postjump	l Shell	i Shell	s shell
1	9.265–9.365	9.39 –9.41	9.501–9.502
2	9.311–9.384	9.425–9.435	9.525–9.526
3	9.265–9.440	9.466–9.471	9.5253–9.5257
4	9.24 –9.402	9.435–9.445	9.451–9.452
5	9.311–9.380	9.455–9.448	9.482–9.485
6	9.347–9.401	9.467–9.478	9.521–9.531

NOTE.—Number in each position give the inner and outer radii of the respective shell measured in km. The model is described in § 5.

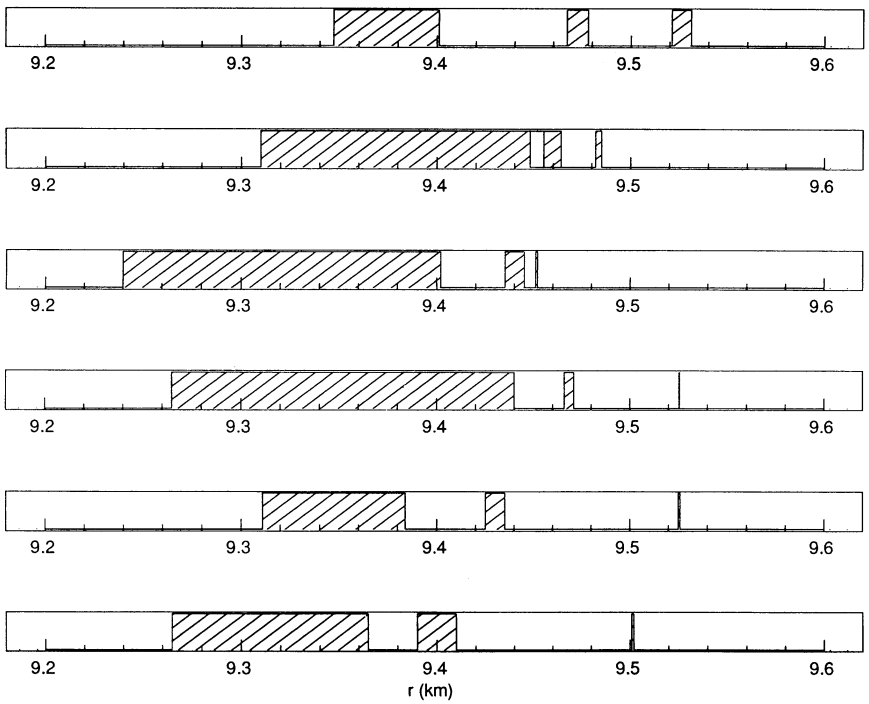

FIG. 3.—Schematic picture of the distribution of relaxation (*shaded regions*) shells is each postjump event of the first six macrojumps in the Vela pulsar

difference between the superfluid and the normal components in the i and s shells is lower than in the l shell, since τ_s, $\tau_i \ll \tau_l$ (eq. [55]). Therefore the Magnus force, that should be sustained by the pinning forces, in the s and i shells is smaller than in the l-shell by a factor τ_s/τ_l and τ_i/τ_l, respectively.

5. IMPLICATIONS FOR MACROJUMPS

If a macrojump is produced by means of a momentum transfer from the superfluid component, the mechanism responsible for the momentum transfer must produce transfer timescales less than 2 minutes in the case of Vela pulsar (Epstein & Baym 1992). This upper limit for the rise time is set by the observation of the Vela pulsar jump of 1988 (McCulloch et al. 1990; Flanagan 1990).

Next we will show that a shell in the superfluid core can be identified, which has a moment of inertia *and* dynamical coupling times appropriate for generating a jump of the Vela Christmas 1988 type. This shell has a location that is *distinct* from the relaxation shell's location, which is specified by its short dynamical coupling time. Because of the shortness of the rise time the prejump conditions in the relaxation shells are unaffected. Actually, during the rise time the only interacting components are the jump generation shell, (or hereafter g-shell), and the normal component of the star.

Assume that before the jump there is a superfluid spin frequency excess $\Delta v_s > [v_0/\tau_0]\tau_g$, with respect to the equilibrium state departure. This precisely corresponds to the case 2 considered in the previous section. Note that if during the interjump epoch the free flow regime is realized in the g shell, the magnitude of $\Delta v_s/v(0) = \tau_g/\tau_0 < 10^{-8}$ will be extremely small because of the smallness of corresponding dynamical coupling time τ_g. Therefore a mechanism that prevents superfluid relaxation in the g shell in the interjump epoch, and allows it in the jump process should be specified. It might be a pinning-depinning process of vortex clusters to the crust-core interface, in analogy to that proposed by Anderson & Itoh (1975), for the bulk of the crustal superfluid. These aspects will be discussed elsewhere.

The dynamical equation for the *rise process* can be written in the following form

$$v(t) = v(0^-) + \frac{I_g}{I_c}\left(\Delta v_s - \frac{\tau_d}{\tau_0} v_0\right)[1 - e^{-t/\tau_d}] - \frac{v(0)}{\tau_0} t\,, \tag{65}$$

$$\dot{v}(t) = \frac{I_g}{I_c}\left(\Delta v_s - \frac{\tau_d}{\tau_0} v_0\right)\frac{e^{-t/\tau_d}}{\tau_d} - \frac{v(0)}{\tau_0}\,, \tag{66}$$

where $v(0^-)$ is the prejump spin frequency of the crust and I_g is the moment of inertia of the g shell. Here it is assumed $\Delta v_{sg} > [v_0/\tau_0]\tau_g$. Thus $v(t)$ increases with characteristic dynamical coupling timescale τ_g given by the formula (44). At $t \gg \tau_g$, keeping the leading term,

$$v(\infty) - v(0^-) \equiv \Delta v = \frac{I_g}{I_c}\Delta v_s\,, \tag{67}$$

i.e., one finds that accumulated superfluid momentum is transferred to the crust in accord with the momentum conservation condition. Given the ratio I_g/I_c from model calculations and observed Δv one can estimate required prejump Δv_s in the g shell.

From Table 2 it can be seen that the region at the crust core boundary, within the shell $9.62 \leq r \leq 9.64$, in the density range $(1.83\text{–}1.68) \times 10^{14}$ g cm^{-3}, has for the Vela pulsar a mean dynamical coupling time $\tau_g \sim 3$ minutes and moment of inertia $I_g/I_c = 0.02$. The dynamical coupling timescale is close to the upper limit set by the rise time of the Christmas jump. For given parameter I_g/I_c the prejump departure for the superfluid spin frequency according to equation (67) should be $\Delta\nu_s/\nu_0 \sim 5 \times 10^{-5}$, while assuming that the superfluid spin frequency is fixed during the interjump period, ($t_g \sim 2$ yr), the accumulated departure due solely to deceleration of the crust is $\Delta\nu_s/\nu_0 = \dot{\nu} t_g/\nu_0 \sim 10^{-4}$. Thus the magntide of the departure that can be achieved during the interjump epoch is sufficient for driving a jump in the g-shell.

From the discussion above it is evident that the rise process of the jump is analogous to the postjump relaxation process, particularly *both processes are controlled by the dynamical coupling timescale.* The differences are that: (1) In the case of the jump process there is initial superfluid spin frequency excess compared to the equilibrium spin frequencies departure between the normal and superfluid components; the characteristic dynamical times are as a rule remarkably short; (2) In the case of postjump process there is effective superfluid spin frequency reduction with respect to the new dynamical state of the crust, (since jump reduces the equilibrium departure); the dynamical timescales are relatively long.

While there are no reasons to believe that the initial states in cases (1) and (2) are *strongly* correlated with respective dynamical coupling times one would expect that the inverse situation is possible. This implies that, at least for some pulsars, *macrojumps must be observed with long rise times.* Furthermore, an intermediate situation might be possible when the dynamical state is described by *a superposition of rise and relaxation processes with comparable timescales.*

In the next section the observational implications for pulsars other than Vela will be discussed in the context of the present model.

6. IMPLICATIONS OF THE DYNAMICAL MODEL FOR OTHER PULSARS

Dynamical coupling times in the present model are basically temperature independent and therefore the relevant pulsar parameters that change on the evolutionary timescales are the period and its derivatives. Because the dynamical coupling times depend on the rotation period of a pulsar as $\tau_d \sim P^2$, and observed pulsar periods are scattered by more than three orders of magnitude, one of the goals here will be to consider the implications of this dependence for a range of observed pulsar periods. The possibility of accommodating the bulk observational evidence in the present model calculation by finding the appropriate dynamical coupling time and respective moment of inertia for relaxation and rise processes is our next goal. Finally we will discuss the noncanonical jump processes, particularly those with long rise times.

As a guideline in Figure 4 the dynamical coupling times are plotted against the matter density for six different pulsar periods, covering a broad range of observed periods. In Table 4 the macrojumps in pulsars other than Vela are summarized. The rise times are in general represented by upper bounds which are in most cases the interval between the last observation before the jump and the first observation after the jump.

The *Crab pulsar 0531+21*, which is the youngest pulsar in the list, has shown four jumps so far. The exponential relaxation time scales are in the range 2–20 days. The scaling factor for the dynamical coupling times of the Vela and Crab pulsars is $[P_{(\mathrm{Crab})}/P_{(\mathrm{Vela})}]^2 = 0.14$, which translates the range of relaxation timescales observed for the Crab pulsar to the range 14–143 days for the Vela. This range basically covers the short and intermediate response timescales inferred for the Vela pulsar. Thus the different timescales of postjump relaxation in the Vela and Crab pulsars can be attributed to the difference in their periods, provided these stars have approximately the same mass.

The discontinuous rise times for the last two jumps of the Crab pulsar are an hour and less than 2.4 hours, respectively. For the model described in § 4.2 these dynamical coupling times correspond to the densities $\rho \sim 2.17 \times 10^{14}$. The magnitude of the fourth jump implies that $I_g/I_c \sim 4 \times 10^{-2}$ in the g shell (see § 5). According to the present, model the shell in the density interval $2.09 \leq \rho \leq 2.19(\times 10^{14})$ g cm^{-3} can provide enough moment of inertia for a jump of observed magnitude.

TABLE 4

MACROJUMPS IN THE PULSARS OTHER THAN VELA

PSR	P (s)	$\dot{P}$ ($\times 10^{-15}$)	log τ_0 (yr)	Epoch MJD (=JD −2440000)	$\Delta P/P$ ($\times 10^{-9}$)	$\Delta\dot{P}/\dot{P}$ ($\times 10^{-3}$)	τ_{rise} (d)	τ_{decay} (d)	Reference
0355+54.....	0.156	4.391	5.75	6079 ± 7	−5.56	1.8	≤14	...	Lyne (1987)
				6433−6504	−4400.0	62−150	≤71	44	
0525+21.....	3.746	40.045	6.17	2064	−1.3 ± 0.22	4.6 ± 0.9	≤100	...	Downs (1982)
				3834	−0.3 ± 0.08	0.085 ± 0.15	≤100	143 ± 34	
0531+21.....	0.033	420.96	3.10	493	−7.26	0.037	≤1.75	2–6	Boynton et al. (1969)
				2448	−(880−1500)	21.5 ± 1.6	≤6	10.2 ± 1.2	Demianski & Proszynski (1983)
				6664.42	−9.2 ± 1	2.5 ± 2	0.042	5.5 ± 0.5	Lyne & Pritchard (1987)
				7768	−61.8	40.0	≤0.1; 0.8; 265	18	Lyne, Smith, & Pritchard (1992)
1641−45.....	0.455	20.09	5.55	3390 ± 63	−191.0 ± 1	1.6 ± 0.5	≤126	...	Manchester et al. (1983)
				6453 ± 35	−803.6 ± 0.1	0.5 ± 0.3	≤69,	200–400	Flanagan (1993)
				7589 ± 4	−1.61 ± 0.04	1.1 ± 0.1	≤8,	200–400	
1737−30.....	0.607	465.67	4.32	6953−7053	−420 ± 20	2.8 ± 0.8	≤100	≥300	McKenna & Lyne (1990)
				7281 ± 2	−33 ± 5	1.7 ± 4.0	≤130	≥70	
				7332 ± 16	−7 ± 5	−1 ± 12	≤50	≥150	
				7458 ± 2	−30 ± 8	0 ± 4	≤100	≥250	
				7607.2 ± 0.2	−600.9 ± 0.6	2.0 ± 0.4	≤32	≥200	
2224+65.....	0.683	9.67	6.05	3034−3109	−1.71 ± 0.02	<6	≤74	...	Backus et al. (1982)

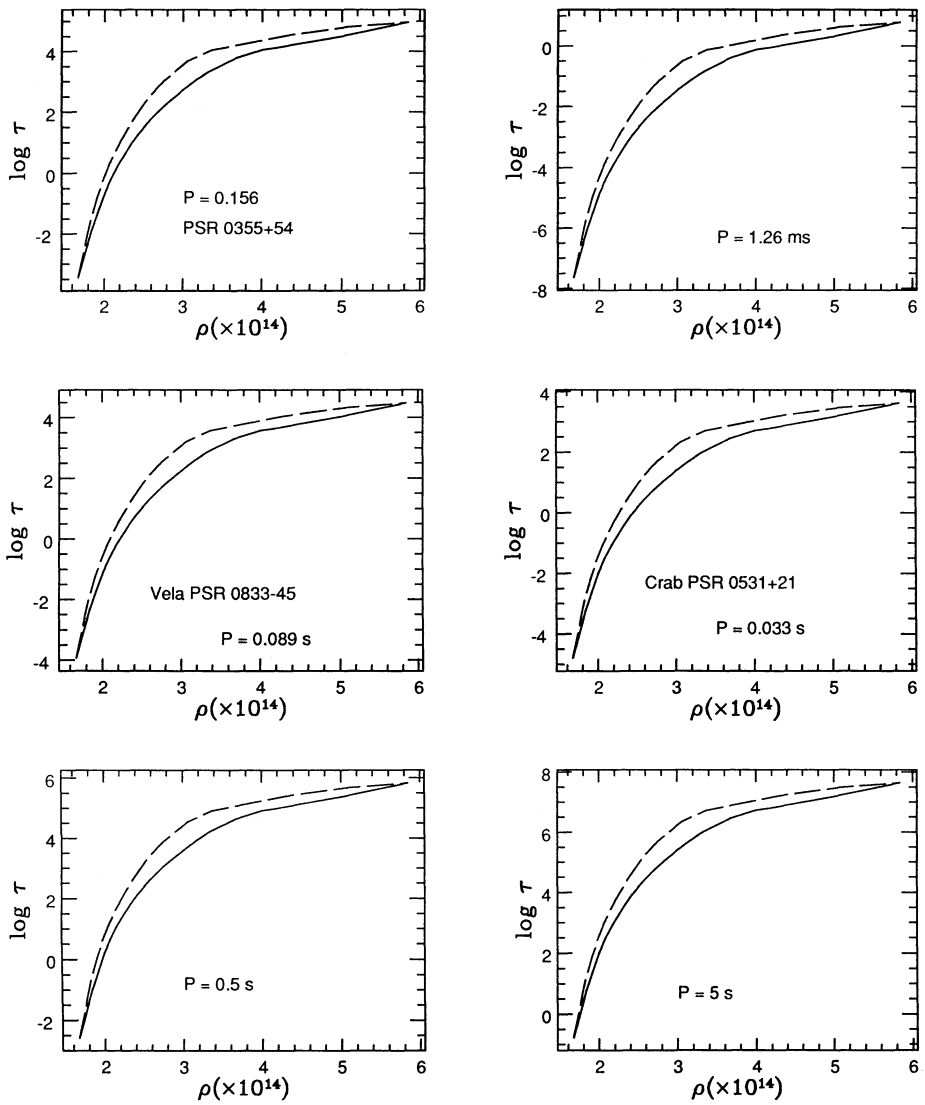

FIG. 4.—Dynamical coupling times are plotted against the matter density for different pulsars. The corresponding effective moment of inertia of different density shells can be found from Table 2. Solid lines are the calculations with proton superconductor parameters given by Baldo et al. (1992), dashed lines—by Wambach et al. (1991).

A new feature revealed in the fourth jump of the Crab pulsar in the long exponential rise in $\dot{\nu}$ with timescales 0.8 and 265 days (Lyne et al. 1992). The underlying mechanism for exponential rises can be identical with the process leading to the discontinuous jump: Both processes are described by equation (65) with the only difference being the dynamical coupling times. Indeed, if initial conditions are such that $\Delta\nu^{(ex)} > \Delta\nu$, in a local region with specific coupling time, (e.g., due to the pinning of vortex clusters to the crust-core interface or vortex cluster number fluctuations), then what will be observed after the jump is an exponential rise process with the respective dynamical coupling time. In other words, the g shell, where the coupling times are short, produces a short scale (unresolved) rise which is the actual jump, while other shells with analogous initial conditions will produce exponential rises on their dynamical coupling times. The rise time of 265 days revealed by Lyne et al. (1992) corresponds to the shell with density $\rho \sim 3.6 \times 10^{14}$ g cm^{-3} in the present model. For the Vela pulsar this shell would have coupling timescale $\sim$1900 days, which is a factor of 2 larger than a typical interjump period for that pulsar.

PSR 1737−30 showed five macrojumps in a period of 3 years (McKenna & Lyne 1990). The age of this object is comparable to the Vela, however their dynamical characteristics, (P, $\dot{P}$), are different.[5] The spin frequency derivative of PSR 1737−30 is a factor of 10 smaller than that of the Vela, which implies that the angular momentum accumulation must be roughly by this factor lower than in the Vela pulsar. Therefore, the remarkable shortness of the interjump periods in this pulsar suggests that each jump is caused by a

[5] The fact that the ages of PSR 1737−30 and Vela are close indirectly suggests that the internal temperatures of these pulsars are similar; therefore, the remarkable difference in their dynamical behavior cannot be attributed to their temperature.

different g shell. (In fact observation of different rise times in future jumps, which, as pointed out by McKenna & Lyne (1990), is facilitated by the short interjump intervals, would indicate if different shells are involved in producing the jumps). The observational lower bound for the rise time in this pulsar is 30 days which corresponds to a shell with density $\rho \sim 2.17 \times 10^{14}$ g cm^{-3}.

The dynamical timescales for a pulsar period $P = 0.5$ s, which is close to that of PSR 1737−30 are given in Figure 4. The scaling factor for the dynamical coupling times of the Vela and PSR 1737−30 is $[P_{(1737-20)}/P_{(\text{Vela})}]^2 = 46.5$, which translates the range of short and intermediate relaxation timescales of the Vela pulsar to the range 300–5500 days for PSR 1737−30. Thus the relaxation times for this pulsar can be much larger than the interjump epoch, though short term relaxations and rises are not excluded by the model calculation (see Fig. 4). Finally note that for this pulsar a large part of the superfluid core at densities $\rho \geq 4 \times 10^{14}$ is actually decoupled from the normal component on the evolutionary timescales.

PSR 1641−45 has been observed to exhibit three macrojumps (Manchester et al. 1983; Flanagan 1993). The shortest unresolved rise timescale in the case of the third jump is 8 days, which according to the model calculations corresponds to densities $\rho \simeq 2.1 \times 10^{14}$ g cm^{-3}. After the second and third jumps the spin frequency derivative shows wandering with a timescale of 200–400 days, with a general long term increase in its magnitude. The wandering process suggests a superposition of responses from rise and relaxation shells with indicated timescales. The interpretation of the long rise processes is analogous to that in the case of the Crab pulsar, i.e., this is a rise process in the shells with a long dynamical coupling time. For PSR 1641−45 the timescales $\simeq$400 days corresponds to the densities $\rho \simeq 2.6 \times 10^{14}$ g cm^{-3}. No short term exponential relaxation can be separated from the long term timing noise (Flanagan 1993). Such relaxation components cannot be excluded on the basis of model calculations, (see Fig. 4).

Two macrojumps have been observed in the PSR 0355+54 (Lyne 1987), which differ from each other essentially by magnitudes of ΔP and $\Delta \dot{P}$. The rise time for the first smaller jump is less than 14 days, which can be associated with a shell with density $\rho \leq 2.5 \times 10^{14}$ g cm^{-3}. The rise time for the second large jump is less than 71 days, can be produced by any shell with density below 2.8×10^{14} g cm^{-3}. The magnitude of this jump is quite large, but the uncertainty in its occurrence time does not allow for determining the moment of inertia of corresponding shell.

A 44 day exponential relaxation was deduced for the second jump (Lyne 1987). The effective moment of inertia of the superfluid shell, under analogous assumptions about the initial conditions, as in the case of the relaxation shells in Vela (see eqs. [60] and [61]), is $I_s/I_c = (\Delta\dot{\nu}\tau)/\Delta\nu = [0.1\text{–}0.28]$, the lower and upper limits corresponding to the respective limits in $\Delta\dot{\nu}$. In this estimate the remnant change $\Delta\dot{\nu}/\dot{\nu} = 6.2 \times 10^{-3}$ was subtracted from the macrojump value of $\Delta\dot{\nu}/\dot{\nu}$.

The lower value for I_s/I_c can be obtained by averaging in a density shell $2.34 \leq \rho \leq 2.67 \times 10^{14}$ g cm^{-3} corresponding to the coupling time range $9 \leq \tau \leq 90$ days. Clearly a larger averaging region is required for accounting for larger numbers. There are two alternative possibilities: A larger fraction of moment of inertia of the star must be decoupled from the observable crust, than assumed in the present model. This will reduce I_c. Different prejump initial conditions are required, namely the spin frequency of the superfluid must be *lower* than that implied by equilibrium departure. This will increase the effective $\Delta\nu$. Observation of a jump with smaller uncertainty interval in the occurrence of jump will allow to draw more definitive conclusions on the shells involved in the postjump relaxation in this pulsar.

Most of the characteristic parameters of the single jump observed in PSR 2224+65 (Backus, Taylor, & Damashek 1982) are rather uncertain. This pulsar has a period close to PSR 1737−30, and therefore a similar spectrum of dynamical coupling times. However the period derivatives of these pulsars, and consequently their estimated ages, differ by two orders of magnitude, implying that the jump occurrence rate in PSR 2224+65, should roughly be two orders of magnitude less than in PSR 1737−30.

PSR 0525+21, with period $P \sim 4$ s is the slowest pulsar which exhibited macrojumps (Downs 1982). The scaling factor for dynamical coupling times with respect to the Vela pulsar is 1.8×10^3! The uncertainty in the timescale of the rise process for this pulsar is $\leq$100 days. These timescales correspond to the density shell $\rho < 2 \times 10^{14}$ g cm^{-3}. The maximum value of moment of inertia allowed for the generation shell by the present model is $I_s/I_c \sim 0.05$. The largest value of $\Delta\dot{\nu}/\dot{\nu} \simeq 0.005$ is however an order of magnitude smaller than that provided by the present model using the relation $I_s/I_c \sim \Delta\dot{\nu}/\dot{\nu}$. Note also that, a large fraction of the superfluid core at densities $\rho > 2.2 \times 10^{14}$ g cm^{-3} is coupled to the observable crust on evolutionary timescales, which effectively reduces the moment of inertia of the crust. The observed 143 day relaxation process can be produced by a shell with density $\rho \simeq 2 \times 10^{14}$ g cm^{-3}. Future observations which will allow reduction of the uncertainty in the jump occurrence times and which will reveal further exponential relaxation in this particular pulsar can place severe constraints on the present model. The lower bound on the dynamical coupling times are several days.

Millisecond pulsars have not been observed to exhibit macrojumps and the level of their timing noise is remarkably low. The dynamical coupling times for a millisecond pulsar with $P = 1.26$ ms are shown in Figure 4. An interesting *negative* prediction of the present model for the millisecond pulsars is that, *millisecond pulsars cannot exhibit long-term—larger than a few days—postjump relaxations or rises.*

7. CONCLUSIONS

We have presented a dynamical model of superfluid core rotation in pulsars. General dynamical equations of the nonstationary rotation of superfluid systems were derived taking into account the spatial dependence of vortex viscous friction. Particularly, we found solutions of coupled integro-differential equations describing the postjump response by applying a perturbation theory with respect to the small parameter of the problem—the ratio of the superfluid moment of inertia to that of the normal component. By summing infinite series of the perturbation expansion an exact result for the postjump behavior with spatial dependence of friction is found.

The dynamical coupling times of the superfluid core to the normal component of the star produced by vortex cluster friction are proportional to the square of the period of pulsar. We discuss several implications of this dependence for a large range of pulsar periods. Particularly we find that for extremely slow pulsars, like PSR 0525+21 with period $P \sim 4$ s, relaxation and rise processes shorter than several days cannot be understood in the present model. In the opposite limit of rapidly rotating millisecond pulsars we

find that the superfluid cores are coupled to the normal component on short timescales and relaxations or rises on times larger than few days will be in contradication with present model.

The dynamical coupling times are continuous functions of the matter density. However for practical applications we introduced the so called shell model, where the entire core is divided into a number of dynamically independent shells with an averaged relaxation time constant.

Let us next summarize the postjump and model analysis:

1. Within standard parameters of neutron stars, (equation of state of WFF, and a $M = 1.4\ M_{\odot}$ star), and realistic microscopic input (Baldo et al. 1992) we were able to identify regions in the superfluid cores with observed time constant and appropriate moment of inertia.

2. The first six jumps of the Vela pulsar can be described in terms of short and intermediate exponential relaxations, which are superposed upon a long-term linear relaxation. This behavior is naturally implied by the dynamical equations for superfluid regions in *the free vortex flow regime with spatial dependence of vortex friction.* Particularly, the long-term response is derived from an exponential response caused by a shell with the dynamical coupling time larger than the characteristic timescale of macrojump relaxation process.

3. The shell model is a rough approximation to a continuum model where the whole spectrum of timescales is present with appropriate weighting determined by the prejump state of superfluid core. However the shell model appears to be a useful tool in revealing the possibilities provided by the models of neutron stars and microscopic input. Fits to the postjump data using a continuum postjump model will actually show the limits and accuracy of the shell model.

Present model calculations show that the short dynamical coupling times ($\tau \sim 2$) min. required for the rapid momentum transfer for generation of the Christmas 1988 marcojump in the Vela pulsar are attained in the superfluid core layers close to the crust-core interface. The moment of inertia of this shell appears to be consistent with the magnitude of the microjump. It is suggested that the mechansim for producing the jump might be pinning of the vortex clusters to the crust-core interface as in the case of rotating superfluid helium, and in analogy to the bulk pinning in the crust as developed by Anderson & Itoh (1975), and Alpar et al. (1984a). The details of the boundary pinning will be given in a subsequent publication.

Finally, it is proposed that the new class of timing irregularities—the postjump long exponential rises, as observed in the Crab pulsar (Lyne et al. 1992) and in PSR 1641−45 (Flanagan 1993), are in fact quite analogous to the macrojump generation processes, but are caused by the shells with long dynamical coupling times. In other words, it shows that any superfluid shells that will have superfluid spin frequency excess with respect to the equilibrium at the moment of the macrojump will cause exponential rise on the respective dynamical coupling timescale.

We conclude that within standard range of parameters of neutron stars and microscopic physical input the complex of macrojump processes and postjump relaxations can be understood in terms of dynamics of superfluid cores in pulsars.

We are thankful to F. Weber for providing unpublished data on the internal structure and composition of models of neutron stars, to Claire S. Flanagan and P. M. McCulloch for useful communications, and to I.Wasserman for useful discussions. The work of A. S. and D. S. was in part supported by a NASA grant NAGW-3591 to Cornell University. The work of J. M. C. was supported by NSF grant AST 92-18075. J. M. C. and Y. T. were supported by the National Astronomy and Ionosphere Center, NSF grant AST 89-20849.

REFERENCES

Alpar, M. A., Anderson, P. W., Pines, D., & Shaham, J. 1984a, ApJ, 276, 325
Alpar, M. A., Chau, H. F., Cheng, K. S., & Pines, D. 1993, ApJ, 409, 345
Alpar, M. A., Langer, S. A., & Sauls, J. A. 1984b, ApJ, 282, 533
Anderson, P. W., & Itoh, N. 1975, Nature, 256, 25
Backus, P. R., Taylor, J. H., & Damashek, M. 1982, ApJ, 255, L63
Baldo, M., Cugnon, J., Lejeune, A., & Lombardo, U. 1992, Nucl. Phys. A, 536, 349
Baym, G., Epstein, R. I., & Link, B. 1990, Physica B, 178, 1
Baym, G., Pethick, C. J., Pines, D., & Ruderman, M. A. 1969, Nature, 224, 872
Bildsten, & L., Epstein, R. 1989, ApJ, 342, 951
Boynton, P. E., Groth, E. J., Partridge, R. B., & Wilkinson, D. T. 1969, IAU Circ. 2179
Cheng, K. S., Alpar, M. A., Pines, D., & Shaham, J. 1988, ApJ, 330, 835
Cordes, J. M., Downs, G. S., & Krause-Polstorff, J. 1988, ApJ, 330, 847
Demianski, M, & Proszynski, M. 1983, MNRAS, 202, 437
Downs, G. S. 1982, ApJ, 257, L67
Epstein, R. I., & Baym, G. 1992, ApJ, 387, 276
Feibelman, P. J. 1971, Phys. Rev. D, 4, 1589
Flanagan, C. S. 1990, Nature, 345, 416
———. 1993, MNRAS, 260, 643
Greenstein, J. 1975, ApJ, 200, 281
Hamilton, P. A., King, E. A., McConnell, D., & McCulloh, P. M. 1989, IAU Circ. No. 3729
Jones, P. B. 1990, MNRAS, 246, 315
———. 1992, MNRAS, 257, 501
Krasnov, Yu. K. 1977, Soviet Phys.–JETP Lett., 46, 181
Link, B., Epstein, R. I., & Baym, G. 1993, ApJ, 403, 285
Lorenz, C. P., Ravenhall, D. G., & Pethick, C. J. 1993, Phys. Rev. Lett., 70, 379
Lyne, A. G. 1987, Nature, 326, 569
Lyne, A. G., & Pritchard, R. S. 1987, MNRAS, 229, 223
Lyne, A. G., Smith, F. G., & Pritchard, R. S. 1992, Nature, 359, 706
Manchester, R. N., Newton, L. M., Hamilton, P. A., & Goss, W. M. 1983, MNRAS, 202, 269
McCulloch, P. M., Hamilton, P. A., McConnel, D., & King, E. A. 1990, Nature, 346, 822
McKenna, J., & Lyne, A. G. 1990, Nature, 343, 349
Ruderman, M. A. 1969, Nature, 223, 597
Ruderman, M. A., & Sutherland, P. G. 1974, ApJ, 190, 137
Sauls, J. A., Stein, D. L., & Serene, J. W. 1982, Phys. Phys. Rev. D, 25, 967
Sedrakian, A. D., & Sedrakian, D. M. 1992, Soviet Phys.–JETP Lett., 75, 395
———. 1995, ApJ, 447, in press (Paper I)
Wambach, J., Ainsworth, T., & Pines, D. 1991, in Neutron Stars: Theory and Observations ed. J. Ventura & D. Pines (Dordrecht: Kluwer), 37
Weber, F. 1992, Habilitation thesis, Univ. of Munich
Wiringa, R. B., Fiks, V., & Fabrocini, A. 1988, Phys. Rev. C, 38, 1010 (WFF)